Monomeric Cyclopentadienylnickel Methoxo and Amido Complexes: Synthesis, Characterization, Reactivity, and Use for Exploring the Relationship between H–X and M–X Bond Energies

Patrick L. Holland,[†] Richard A. Andersen,*,[†] Robert G. Bergman,*,[†] Jinkun Huang,[‡] and Steven P. Nolan[‡]

Contribution from the Department of Chemistry, University of California, Berkeley, California 94720, and the Department of Chemistry, University of New Orleans, New Orleans, Louisiana 70148

Received June 4, 1997[⊗]

Abstract: Reactive monomeric amido and methoxo complexes, Cp*Ni(PEt₃)NHTol and Cp*Ni(PEt₃)OMe, have been synthesized and fully characterized. The former is the first monomeric 18-electron nickel amide to be synthesized and the latter is the first structurally characterized monomeric nickel methoxide complex. The amido complex Cp*Ni-(PEt₃)NHTol reacts with various Brønsted acids (HX) to produce complexes of the type Cp*Ni(PEt₃)X (X = NHAr, OR, Osilica, SR), and compounds with hydridic hydrogens to give the hydridonickel complex Cp*Ni(PEt₃)H. The polarity of Ni–N and Ni–O bonds is also demonstrated by reactions with alkali metal salts and trimethylsilyl chloride, and by the crystallographic and NMR characterization of phenol adducts of Cp*Ni(PEt₃)OTol. The phosphine ligands in Cp*Ni(PEt₃)X (X = OTol, SAr) compounds exchange with PMe₃ through an associative mechanism; the rate increases with the electronegativity of X. The thermodynamics of reactions interconverting Cp*Ni(PEt₃)X + HX′ and Cp*Ni(PEt₃)X′ + HX have been analyzed using solution equilibrium studies and calorimetry. Instead of being 1:1, the correlation between H–X and M–X bond energies shows a marked preference for nickel binding to more electronegative ligands. This preference is not specific to nickel: examples of similar thermodynamic preferences occur throughout transition metal chemistry. These results may be attributable to a large electrostatic component in the bonding between Ni and X. This qualitative *E–C* model explains the reactivity, thermodynamics, and phosphine exchange rates of this series of nickel complexes, and may be general to many metal–ligand bonds.

Introduction

Late transition metal compounds with anionic nitrogen and oxygen ligands are important intermediates in industrial[1,2] and biological[3] processes. While many new complexes of this type have been synthesized recently by our group[4–7] and others,[8–21]

[†] University of California, Berkeley.
[‡] University of New Orleans.
[⊗] Abstract published in *Advance ACS Abstracts,* December 15, 1997.
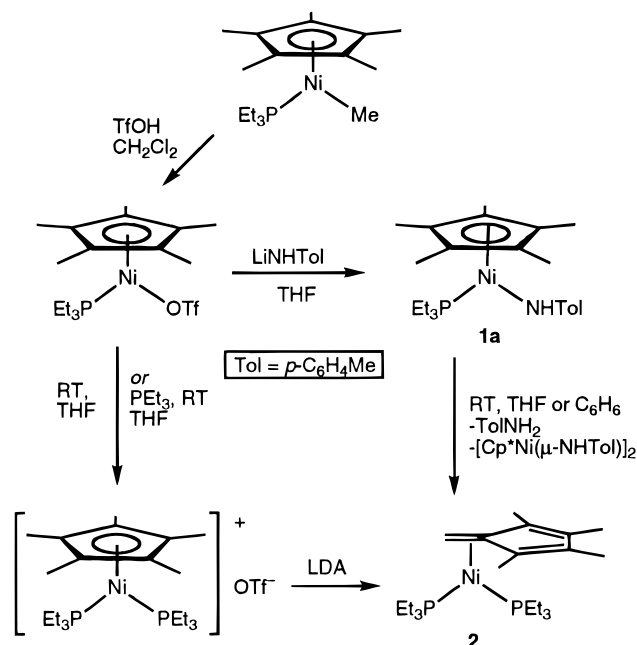(1) Roundhill, D. M. *Chem. Rev.* **1992,** *92,* 1.
(2) Bryndza, H. E.; Tam, W. *Chem. Rev.* **1988,** *88,* 1163.
(3) For leading references, see: Holm, R. H.; Kennepohl, P.; Solomon, E. I. *Chem. Rev.* **1996,** *96,* 2239, and other articles in the same issue.
(4) Bergman, R. G. *Polyhedron* **1995,** *14,* 3227.
(5) Kaplan, A. W.; Bergman, R. G. *Organometallics* **1997,** *16,* 1106.
(6) For related chemistry of a late-metal fluoride, see: Veltheer, J. E.; Burger, P.; Bergman, R. G. *J. Am. Chem. Soc.* **1995,** *117,* 12478.
(7) Holland, P. L.; Andersen, R. A.; Bergman, R. G. *J. Am. Chem. Soc.* **1996,** *118,* 1092.
(8) Kawataka, F.; Kayaki, Y.; Shimizu, I.; Yamamoto, A. *Organometallics* **1994,** *13,* 3517.
(9) Brunet, J.-J.; Commenges, G.; Neibecker, D.; Phillippot, K.; Rosenberg, L. *Inorg. Chem.* **1994,** *33,* 6373.
(10) Koo, K.; Hillhouse, G. L. *Organometallics* **1995,** *14,* 4421.
(11) VanderLende, D. D.; Abboud, K. A.; Boncella, J. M. *Inorg. Chem.* **1995,** *34,* 5319.
(12) Bennett, M. A.; Jin, H.; Li, S.; Rendina, L.; Willis, A. C. *J. Am. Chem. Soc.* **1995,** *117,* 8335.
(13) Grushin, V. V.; Alper, H. A. *Organometallics* **1996,** *15,* 5242.
(14) Driver, M. S.; Hartwig, J. F. *J. Am. Chem. Soc.* **1996,** *118,* 7217.
(15) Mann, G.; Hartwig, J. F. *J. Am. Chem. Soc.* **1996,** *118,* 13109.
(16) Woffe, J. P.; Wagaw, S.; Buchwald, S. L. *J. Am. Chem. Soc.* **1996,** *118,* 7215.
(17) Galanski, M.; Keppler, B. K. *Inorg. Chem.* **1996,** *35,* 1709.
(18) Li, J. J.; Li, W.; Sharp, P. R. *Inorg. Chem.* **1996,** *35,* 604.
(19) Bücken, K.; Koelle, U.; Pasch, R.; Ganter, B. *Organometallics* **1996,** *15,* 3095.

the factors controlling the nature of M–N and M–O bonds are still not well understood.

In this work, new examples of monomeric nickel amido and alkoxo complexes are presented. Their reactivities are governed by the high polarity of their Ni–X bonds. In most cases, the products of the reactions have been crystallographically characterized; the structural details are presented separately with a study of effects on the ancillary pentamethylcyclopentadienyl (Cp*) ligand.[22] In addition to studying the reactivity of these compounds toward X–H bonds, we have used equilibrium studies and substituent effect correlations to gain insight into the electronic nature of the Ni–X bond. These results run counter to the current model for predicting late metal–X bond energies and we offer a more general qualitative model based on *E–C* theory. The new model follows from trends observed in the reactivity, stability, and thermodynamic preferences of all covalent bonds between late metals and ligands, and it shows promise of further understanding of how electronic effects change M–X bond energies.

Results

Synthesis of a Nickel Triflate. The synthesis of Cp*Ni-(PEt₃)X complexes proceeded from the conveniently prepared

---
(20) Canty, A. J.; Jin, H.; Roberts, A. S.; Skelton, B. W.; White, A. H. *Organometallics* **1996,** *15,* 5713.
(21) Klein, H.-F.; Bickelhaupt, A.; Lemke, M.; Sun, H.; Brand, A.; Jung, T.; Röhr, C.; Flörke, U.; Haupt, H.-J. *Organometallics* **1997,** *16,* 668.
(22) See the accompanying paper. Holland, P. L.; Smith, M. E.; Andersen, R. A.; Bergman, R. G. *J. Am. Chem. Soc.* **1997,** *119,* 12815.
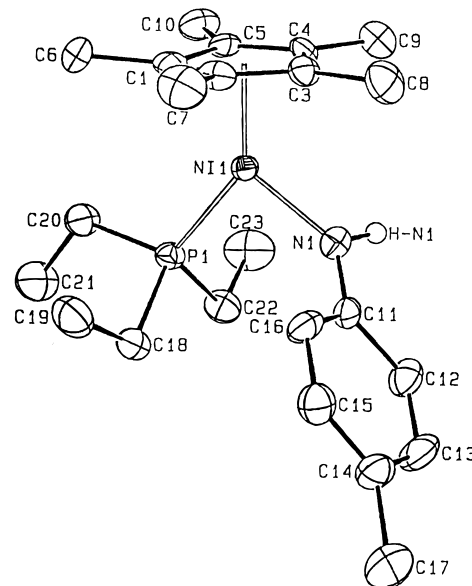
Scheme 1

Figure 1. ORTEP diagram of one of the two independent molecules of **1a** in the unit cell, using 50% probability surfaces. Selected distances and angles for both molecules: Ni−N = 1.903(5), 1.903(5) Å; Ni−Cp(centroid) = 1.763, 1.762 Å; Cp−Ni−P = 139.97, 142.08°; Cp−Ni−N = 126.92, 126.27°; P−Ni−N = 92.9(2), 91.4(2)°; P−Ni−N−C (dihedral) = 74.8(5), 72.3(5)°.

alkyl complex Cp*Ni(PEt$_3$)Me (Scheme 1).[22] This methyl complex was resistant to protonation of the methyl ligand by anilines or phenols, but the stronger acid TolSH reacted with Cp*Ni(PEt$_3$)Me to give the thiolate complex Cp*Ni(PEt$_3$)STol (**5**), and triflic acid reacted with Cp*Ni(PEt$_3$)Me to give the red triflate complex Cp*Ni(PEt$_3$)OTf. Although this triflato-nickel complex has been fully characterized, it was resistant to isolation in good yield, so crude Cp*Ni(PEt$_3$)OTf was usually used in subsequent syntheses.

In dichloromethane solution, the triflato complex readily reacts with Lewis bases such as THF, *p*-toluidine, or acetonitrile, as indicated by a change in color from red to yellow. Over a period of days, Cp*Ni(PEt$_3$)OTf or its base adducts decompose in THF solution to give the bis(phosphine) complex [Cp*Ni(PEt$_3$)$_2$][OTf] as the only isolable product (Scheme 1). When 1 equiv of PEt$_3$ is added to Cp*Ni(PEt$_3$)OTf, the bis(phosphine) complex can be isolated in 61% yield.[23] The X-ray crystal structure of [Cp*Ni(PEt$_3$)$_2$][OTf] shows that the triflate ligand is outer sphere.[22]

Synthesis of a Monomeric Nickel Amide. Crude Cp*Ni(PEt$_3$)OTf was treated with LiNHTol (Tol = *p*-C$_6$H$_4$Me); workup afforded Cp*Ni(PEt$_3$)NHTol (**1a**) in typical yields of 50−60% from the methylnickel complex. The product displays a characteristic resonance in its ^{1}H NMR spectrum at δ −1.5 ppm for the nitrogen-bound proton. The solid-state structure of **1a** was determined by X-ray crystallography; an ORTEP diagram is shown in Figure 1. There are two crystallographically independent, but structurally similar, molecules in the asymmetric unit (bond distances and angles to Ni are within 0.01 Å and 3°, respectively). The nickel−nitrogen distances are both 1.903(5) Å; this distance is longer than those in the low-coordinate nickel amides prepared by Power,[24,25] but shorter than that in the only crystallographically characterized square-planar terminal amidonickel complex.[11] Notably, the nitrogen atoms are planar in **1a**; this geometry presumably arises from

delocalization of the nitrogen lone pair into the aromatic ring. The torsion angles P−Ni−N−C are 72° and 75°, indicating that the filled nitrogen *p* orbital of the amido ligand avoids interaction with the HOMO of the metal fragment, which is perpendicular to the Ni−P−X plane.[26] In a series of analogous complexes Cp*Ni(PEt$_3$)X (X = TolNH, TolO, TolS, PhCH$_2$), the geometries about the metal center and X ligand are quite similar,[22] suggesting that steric effects, not π interactions, control the molecular conformation.

The resonances for the aryl protons in the proton NMR spectrum of **1a** were broad at room temperature; the signals sharpened to two doublets at higher temperatures, and decoalesced to a complicated series of signals at lower temperatures ($T_c \approx$ −42 °C; $\Delta G^{\ddagger}$ = 11 kcal/mol).[27,28] This phenomenon was accompanied by decoalescence of the signals corresponding to the PEt$_3$ methylene protons, which become inequivalent in the low-temperature regime, indicating that this fluxionality corresponds to hindered rotation about the Ni−N bond.

Thermal decomposition of **1a** over 1 d at room temperature in benzene-d_6 solution, as monitored by ^{1}H NMR spectroscopy, produces a mixture of TolNH$_2$, [Cp*Ni(μ-NHTol)]$_2$, and the new nickel(0) tetramethylfulvene complex (C$_5$Me$_4$CH$_2$)Ni(PEt$_3$)$_2$ (**2**) (Scheme 1). No intermediates are observed in the ^{31}P{^{1}H} NMR spectra of decomposing solutions of **1a**. However, this decomposition may be envisioned as proceeding through deprotonation of the Cp* ligand by the amido ligand to produce TolNH$_2$ and (C$_5$Me$_4$CH$_2$)Ni(PEt$_3$), which could abstract a phosphine ligand from another molecule of **1a** to produce **2** and a second intermediate, Cp*Ni(NHTol), which quickly dimerizes to [Cp*Ni(μ-NHTol)]$_2$, even at low temperature.[7]

It has not been possible to isolate **2** cleanly from the mixtures obtained by decomposition of **1a**. Deprotonation of [Cp*Ni(PEt$_3$)$_2$][OTf] with LDA, though, can be used to give **2** in an isolable form (Scheme 1). Complex **2** has a characteristic AB

(23) Jolly, P. W. η-Cyclopentadienyl Complexes. In *Comprehensive Organometallic Chemistry*, 1st ed.; Wilkinson, G., Ed.; Pergamon: New York, 1982; Vol. 6, p 189.

(24) Hope, H.; Olmstead, M. M.; Murray, B. D.; Power, P. P. *J. Am. Chem. Soc.* **1985**, *107*, 712.

(25) Bartlett, R. A.; Chen, H.; Power, P. P. *Angew. Chem., Int. Ed. Engl.* **1989**, *28*, 316.

(26) Albright, T. A.; Burdett, J. K.; Whangbo, M.-H. *Orbital Interactions in Chemistry*; Wiley: New York, 1985.

(27) Legzdins, P.; Jones, R. H.; Phillips, E. C.; Lee, V. C.; Trotter, J.; Einstein, F. W. B. *Organometallics* **1991**, *10*, 986.

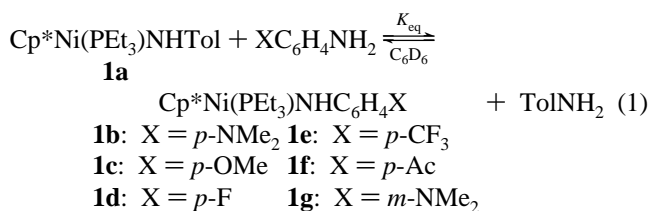(28) Thomas, W. A. *Annu. Rev. NMR Spectrosc.* **1968**, *1*, 43.

Table 1. Equilibrium Constants for Amide/Amine Exchanges[a]

Ar = XC_6H_4	K_{eq} (est. error)	$\Delta G°$ (kcal/mol)
p-NMe$_2$ (**1b**)	0.21 (0.02)	+0.9 (0.1)
p-OMe (**1c**)	0.50 (0.05)	+0.4 (0.1)
p-Me (**1a**)	1	0
p-F (**1d**)	2.2 (0.3)	−0.5 (0.1)
p-CF$_3$ (**1e**)	400 (50)	−3.5 (0.1)
p-Ac (**1f**)	2 (1) × 10^3	−4.5 (0.3)
m-NMe$_2$ (**1g**)	1.1 (0.2)	−0.1 (0.1)

[a] K_{eq} values at room temperature for the reactions in eq 1 were determined by integration of ^{1}H and ^{31}P{^{1}H} NMR spectra: see Experimental Section for details.

pattern in its ^{31}P{^{1}H} NMR spectrum, showing that the phosphorus atoms are inequivalent. A molecule very similar to **2**, (C$_5$Me$_4$CH$_2$)Pd(PMe$_3$)$_2$, has been crystallographically characterized, and it binds through the *exo* double bond.[29] The NMR data of **2** also substantiate *exo* binding: the resonance for the methylene protons in the ^{1}H NMR spectrum has an upfield chemical shift of δ 2.05 ppm, and the coupling pattern is consistent with coupling of these protons to both phosphorus atoms.

Solutions containing other arylamido complexes could be generated from **1a** by reaction with the appropriately substituted aniline. The equilibrium constants (Table 1) for the equilibria indicated in eq 1 were measured by ^{1}H NMR spectroscopy in

$$\text{Cp*Ni(PEt}_3)\text{NHTol} + XC_6H_4NH_2 \underset{C_6D_6}{\overset{K_{eq}}{\rightleftharpoons}}$$
$$\textbf{1a}$$
$$\text{Cp*Ni(PEt}_3)\text{NHC}_6H_4X \quad + \text{ TolNH}_2 \quad (1)$$

1b: X = p-NMe$_2$ **1e**: X = p-CF$_3$
1c: X = p-OMe **1f**: X = p-Ac
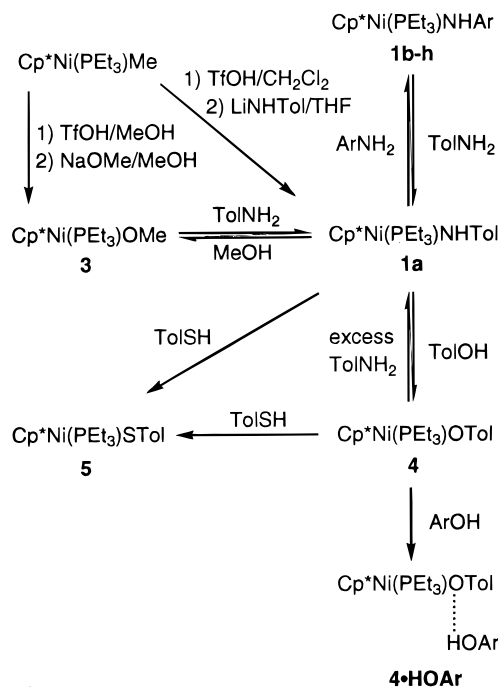**1d**: X = p-F **1g**: X = m-NMe$_2$

benzene-d_6 solution and were independent of the concentrations of reagents used. The ability to isolate *para*-substituted arylamidonickel complexes **1b−g** from this reaction was often hampered by small equilibrium constants and/or volatility differences between the anilines; this could be overcome by using lithium amides in reactions analogous to that used to synthesize **1a**, or from the methoxide as described below.

Synthesis of a Monomeric Nickel Methoxide. When a methanolic solution of Cp*Ni(PEt$_3$)Me was treated with triflic acid, followed by addition of NaOMe, the new methoxide complex Cp*Ni(PEt$_3$)OMe (**3**) could be isolated in a yield of 53% (Scheme 2). Complex **3** is even more unstable than **1a**, decomposing to **2** in benzene solution within a few hours at room temperature. The X-ray crystal structure of **3** is presented in the accompanying paper.

The reactivity of **3** is similar to that of **1a**. As a useful reagent for HX exchange, methoxide **3** has an advantage over amide **1a** in that methanol is more volatile than toluidine. In this way, formation of the substituted arylamido species **1b−g** from **3** was easily pushed to completion by evaporation of methanol. However, the lability of the methoxide ligand hinders its isolation in reproducibly high yields. For this reason, we have devoted more time and effort to the reactions of **1a**.

All attempts to synthesize a hydroxo species cleanly have failed, although a product consistent with this formulation may be observed by NMR spectroscopy after adding water to a sample of **1a**. However, the Ni−OH group could not be detected by ^{1}H NMR spectroscopy, and it was impossible to identify the putative hydroxide conclusively.

Scheme 2

Reactions of 1a with Polar Substrates. Complex **1a** quickly reacts with methanol to form an equilibrium mixture of **1a**, **3**, methanol, and TolNH$_2$; the equilibrium constants derived from these reactions were erratic, but always lay between 0.1 and 10.[30] However, when isolated **3** was mixed with p-toluidine, a value of 0.1 was reproducibly derived for K_{eq} as shown in eq 2.
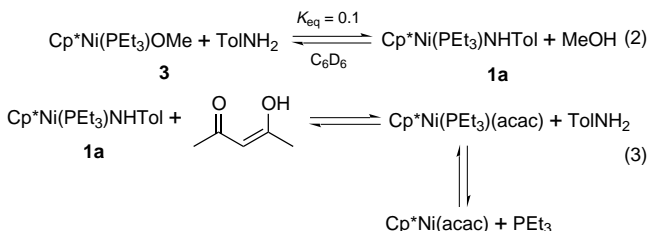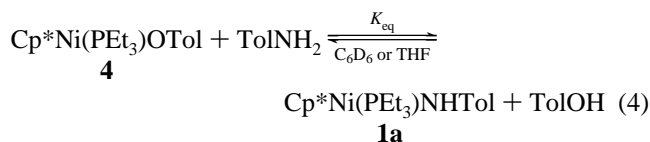

The reaction of **1a** with 2,4-pentanedione, which exists primarily as its enol tautomer at room temperature,[31] also resulted in proton exchange. The product, the previously characterized complex Cp*Ni(η^2-acac)PEt$_3$, exists in equilibrium with Cp*Ni(acac) and free PEt$_3$,[32] so the products were verified by comparison of the ^{1}H NMR spectrum of the mixture to those of the known compounds. Thus, the triethylphosphine ligand of **1a** can be labilized by addition of a chelating alcohol.

More acidic alcohols, when added to **1a**, gave complete conversion to p-toluidine and the corresponding oxygen-bound nickel complex. For example, addition of 1.00 equiv of p-cresol gave only p-toluidine and the new red cresolate complex Cp*Ni-(PEt$_3$)OTol (**4**), as shown by ^{1}H NMR and ^{31}P{^{1}H} NMR spectroscopy (eq 4, Scheme 2). Solution calorimetry of this reaction at 30 °C in benzene solution showed that ΔH_{303K} = −9.4 ± 0.2 kcal/mol. The thermodynamics of this reaction could also be analyzed by spectroscopic techniques. Addition of a large excess (>500 equiv) of p-toluidine to **4** gave a small amount of **1a** visible by ^{1}H and ^{31}P{^{1}H} NMR spectroscopy.

(29) Werner, H.; Crisp, G. T.; Jolly, P. W.; Kraus, H.-J.; Krüger, C. *Organometallics* **1983**, *2*, 1369.

(30) Presumably, the problems with methanol addition lie in the difficulty of completely freeing methanol from trace water.

(31) Hush, N. S.; Livett, M. K.; Peel, J. B.; Willett, G. D. *Aust. J. Chem.* **1987**, *40*, 599.
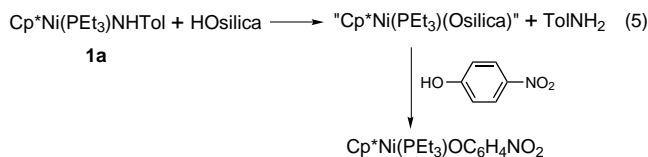
(32) Smith, M. E.; Andersen, R. A. *J. Am. Chem. Soc.* **1996**, *118*, 11119.

$$\text{Cp*Ni(PEt}_3\text{)OTol} + \text{TolNH}_2 \underset{\text{C}_6\text{D}_6 \text{ or THF}}{\overset{K_{eq}}{\rightleftharpoons}}$$
$$\textbf{4}$$

$$\text{Cp*Ni(PEt}_3\text{)NHTol} + \text{TolOH} \quad (4)$$
$$\textbf{1a}$$

The equilibrium constant for eq 4 was determined by ^{1}H NMR spectroscopy to be roughly 10^{-6} in C_6D_6 and roughly 4×10^{-5} in THF-d_8; it was independent of variations in the large amount of p-toluidine added. Because of the difficulty in integrating NMR spectra with a large excess of TolNH$_2$, UV/vis spectroscopy was used to verify this equilibrium constant. This method confirmed that $K_{eq}(C_6H_6) \approx 4 \times 10^{-6}$ and $K_{eq}(\text{THF}) = (4 \pm 2) \times 10^{-5}$; the values in THF solution showed no systematic variation over a 100-fold range of nickel and toluidine concentrations. Although the errors calculated for the equilibrium constants are a large fraction of the values themselves, $\Delta G°$ (proportional to the logarithm of this number) can be determined much more accurately than this implies. Thus, spectroscopic values of $\Delta G°(C_6H_6) = 7.5 \pm 0.8$ kcal/mol and $\Delta G°(\text{THF}) = 6.0 \pm 0.3$ kcal/mol can be derived for eq 4.

The red cresolate complex **4** is much more stable than its amide analogue **1a**. In its crystal structure,[22] the Ni−ligand distances are very similar to those in **1a**, underlining the isosteric character of the OTol and NHTol ligands. The Ni−O distance of 1.889(2) Å is slightly shorter than the Ni−N bond in **1a**, consistent with the difference in covalent radii of N and O. The Ni−O distance in **4** is very similar to that in **3** (1.877(2) Å), and so this distance does not change substantially upon substitution of an aryl for an alkyl substituent on the oxygen atom. However, the aryl C−C distances indicate delocalization of negative charge into the ring, with the C(ring)−C(ipso) distances (av 1.404 Å) longer than the other C(ring)−C(ring) distances (av 1.388 Å), and the C−O distance of 1.330(3) Å being almost as short as that calculated for free LiOPh.[33] Thus, the ground-state geometry of **4** indicates that the Ni−O bond is very polarized.

Silica is another acidic hydroxy compound that could react with **1a** to form Ni−O bonds with loss of p-toluidine. Indeed, silica turned red after treatment with **1a**, indicative of a oxygen-bound Cp*Ni(PEt$_3$) species. The nickel could be removed from the silica in the form of a p-nitrophenolate complex by use of the stronger acid p-nitrophenol. This series of observations is consistent with the production of a complex of the type Cp*Ni-(PEt$_3$)(Osilica) (eq 5).[34]

$$\text{Cp*Ni(PEt}_3\text{)NHTol} + \text{HOsilica} \longrightarrow \text{"Cp*Ni(PEt}_3\text{)(Osilica)"} + \text{TolNH}_2 \quad (5)$$
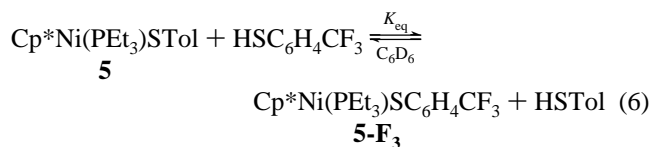$$\textbf{1a}$$

HO—⟨⟩—NO₂

Cp*Ni(PEt$_3$)OC$_6$H$_4$NO$_2$

p-Thiocresol reacted quantitatively with **1a** or **4** to produce the green-brown nickel thiolate complex Cp*Ni(PEt$_3$)STol (**5**) (Scheme 2). This reaction was not reversible, for no achievable amount of p-cresol added to **5** caused observable resonances of **4** to appear in the ^{1}H or ^{31}P{^{1}H} NMR spectra of the solutions. Consistent with this observation, solution calorimetry at 30 °C in benzene showed that reactions between TolSH and **1a** and **4** are exothermic by 23.0 ± 0.2 and 14.0 ± 0.1 kcal/mol, respectively. The crystal structure of **5** has features very similar to those of the arylamide and cresolate complexes.[22] Exchange

---

Scheme 3
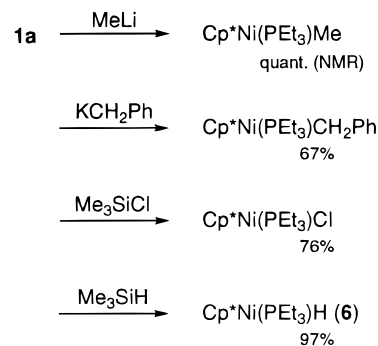
of the thiolate ligand in **5** with p-CF$_3$-substituted thiophenol (eq 6) had an equilibrium constant of only 30, indicating that the thiolate exchanges are less sensitive to substituent effects than the amide exchanges above (eq 1).

$$\text{Cp*Ni(PEt}_3\text{)STol} + \text{HSC}_6\text{H}_4\text{CF}_3 \underset{\text{C}_6\text{D}_6}{\overset{K_{eq}}{\rightleftharpoons}}$$
$$\textbf{5}$$

$$\text{Cp*Ni(PEt}_3\text{)SC}_6\text{H}_4\text{CF}_3 + \text{HSTol} \quad (6)$$
$$\textbf{5-F}_3$$

Even Brønsted acids as weak as anilines reacted with **1a**; as described above, the equilibrium constants for these reactions were measured by ^{1}H NMR spectroscopy. Less acidic amines, such as alkylamines or ammonia, either did not react or caused decomposition of **1a**. In addition, sterically hindered acids, such as diphenylamine and *tert*-butyl alcohol, did not react with **1a**; these results are readily understandable in view of the steric hindrance of the metal center as seen in the crystal structure of **1a**.

Electrophilic organometallic reagents exchanged the amide ligand in **1a** for an alkyl ligand. For example, addition of 1 equiv of methyllithium (as an ether solution) to **1a** caused quantitative conversion to Cp*Ni(PEt$_3$)Me (Scheme 3). The polar Zr−Me bond in Cp$_2$ZrMe$_2$ also reacted to give some of the methylnickel complex, but substantial decomposition also occurred. When a solution of **1a** was treated with a solution of 1 equiv of KCH$_2$Ph, the solution turned green and the complex Cp*Ni(PEt$_3$)CH$_2$Ph could be isolated in 67% yield (Scheme 3). Its X-ray structure[22] shows that the benzyl ligand is in a typical η^1 configuration.[35]

Sources of chloride and bromide invariably transformed **1a** into Cp*Ni(PEt$_3$)X (X = Cl, Br). Thus, LiCl and LiBr, when added in large excess to ether solutions of **1a**, gave partial conversion to the nickel chloride and bromide complexes,[22] respectively. The more convenient chloride source Me$_3$SiCl reacted with **1a** to give quantitative conversion to Cp*Ni(PEt$_3$)-Cl (as judged by ^{1}H NMR spectroscopy). This product was isolated in 76% yield and fully characterized (Scheme 3).

Other H−X bonds reacted with the Ni−N bond of **1a** to give a nickel hydride species: the cleanest reaction of this type was with Me$_3$SiH (Scheme 3). The product, Cp*Ni(PEt$_3$)H (**6**), could be obtained in a yield of 97% from **1a**. Production of **6** from methoxide **3** also proceeded in quantitative yield (as determined by NMR spectroscopy). However, in each of these reactions, it was important to remove residual Me$_3$SiCl from the commercial Me$_3$SiH, because reaction with chlorosilane to produce Cp*Ni(PEt$_3$)Cl (see above) is faster than the reaction

---

(33) Kremer, T.; Schleyer, P. v. R. *Organometallics* **1997**, *16*, 737.

(34) Our group has addressed this issue with other transition metal complexes. See: Meyer, T. Y.; Woerpel, K. A.; Novak, B. M.; Bergman, R. G. *J. Am. Chem. Soc.* **1994**, *116*, 10290.

(35) η^3-Benzyl complexes of nickel are known: Cámpora, J.; Gutiérrez, E.; Poveda, M. L.; Ruiz, C.; Carmona, E. *J. Chem. Soc., Dalton Trans.* **1992**, 1769. Carmona, E.; Paneque, M.; Poveda, M. L. *Polyhedron* **1989**, *8*, 285.
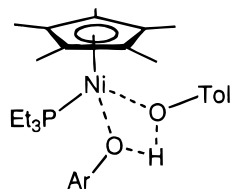
Figure 2. The proposed transition state for aryloxide/phenol exchange.

with the silane. Hydride **6** could also be produced from **1a** using 9-BBN (9-borabicyclononane dimer), but this transformation was not as clean as the silane reaction.

No clean reactions were observed between **1a** and less polar bonds such as the C–C π bonds in acetylenes or ethylene or the H–H bond in dihydrogen. Substrates with activated C–H bonds such as MeCN, $CH_2(CN)_2$, and acetone were observed to react with **1a** to give products with NMR spectra consistent with alkylnickel complexes, but these reactions occurred on the same time scale as decomposition of **1a**, and products were not isolated.

Hydrogen Bonding to 4. If more than 1 equiv of cresol was used in the production of cresolate complex **4** from amido complex **1a**, we were not able to remove the excess cresol, even by crystallization. Unfortunately, we could not successfully characterize the hydrogen-bonded adduct Cp*Ni(PEt₃)OTol· HOTol (**4·HOTol**, Scheme 2) by X-ray crystallography, but NMR experiments gave results characteristic of strong hydrogen bonding. Thus, the ^1H chemical shift of the resonance for the hydroxylic proton in cresol added to **4** shifted from 6.11 ppm (1.5 equiv of cresol) to 5.29 ppm (3 equiv of cresol) upon addition of additional cresol. This observation is indicative of rapid exchange between free and hydrogen-bonded cresol.[36] The infrared spectrum of **4·HOTol** has a very broad peak from 3500–2300 cm⁻¹, indicating weakening of the H–O bond of cresol.

The dynamic behavior of **4·HOTol** was examined using variable-temperature ^1H NMR spectroscopy. When a sample of **4·HOTol** was heated, the resonances corresponding to the cresol and cresolate eventually broadened and coalesced at 95 ± 5 °C. This corresponds to a fluxional process ($\Delta G^\ddagger = 18.5 ± 0.2$ kcal/mol)[27,28] that renders the cresol and cresolate equivalent; presumably, the symmetric transition state for this process resembles Figure 2.[37]

In order to characterize the hydrogen bonding in this type of compound crystallographically, **4** was mixed with 1 equiv of 2,6-dimethylphenol to give Cp*Ni(PEt₃)OTol·HOXyl (**4· HOXyl**). This complex crystallized in space group $P2_1/c$, and refinement proceeded well enough to locate the bridging hydrogen atom and to refine its position and isotropic thermal parameter. An ORTEP diagram of the molecular structure is shown in Figure 3, and important bond distances and angles are listed in Table 2. The O–O distance is 2.627(3) Å, which is in a typical range for alkoxide–alcohol hydrogen bonds.[38] The O(cresol)–H distance is 0.76(3) Å, the O(phenolate)–H distance is 1.89(3) Å, and the O–H–O angle is 166(4)°.

Several bond distances in the nickel cresolate portion of the molecule change from those in **4**[22] in response to the addition of the hydrogen-bonded phenol. For the most part, these appear to be steric in origin, resulting from the larger effective size of the X ligand (X = OTol·HOXyl rather than OTol). Thus, the
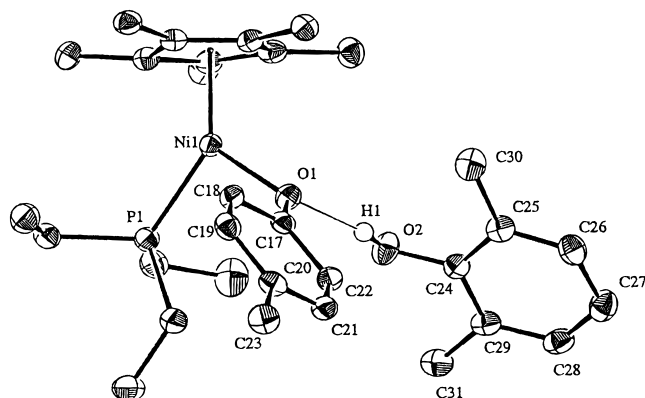
(36) Joesten, M. D.; Schaad, L. J. *Hydrogen Bonding*; Marcel Dekker: New York, 1974.

(37) Simpson, R. D.; Bergman, R. G. *Organometallics* **1993**, *12*, 781.

(38) Cambridge Structural Database: Allen, F. H.; Davies, J. E.; Galloy, J. J.; Johnson, O.; Kennard, O.; Macrae, C. F.; Mitchell, E. M.; Mitchell, G. F.; Smith, J. M.; Watson, D. G. *J. Chem. Inf. Comput. Sci.* **1991**, *31*, 187.

Figure 3. ORTEP diagram of the crystal structure of **4·HOXyl**, using 50% probability surfaces.

Table 2. Selected Bond Distances and Angles in **4·HOXyl**[a]

atoms	distance (Å)	atoms	angle (°)
Ni–Cp	1.755	Cp–Ni–P	140.7
Ni–P	2.1696(8)	Cp–Ni–O(1)	125.4
Ni–O(1)	1.909(2)	P–Ni–O(1)	96.11(6)
Ni–C(1)	2.126(3)	Ni–O(1)–C(17)	122.9(2)
Ni–C(2)	2.199(3)	O(1)–C(17)–C(18)	123.2(2)
Ni–C(3)	2.190(3)	O(1)–C(17)–C(22)	119.4(2)
Ni–C(4)	2.080(3)	C(17)–C(18)–C(19)	121.0(2)
Ni–C(5)	2.153(3)	C(18)–C(19)–C(20)	121.6(3)
O(1)–C(17)	1.350(3)	C(19)–C(20)–C(21)	117.4(2)
C(17)–C(18)	1.401(4)	C(20)–C(21)–C(22)	121.6(2)
C(18)–C(19)	1.393(4)	C(17)–C(22)–C(21)	121.1(2)
C(19)–C(20)	1.395(4)	C(18)–C(17)–C(22)	117.4(2)
C(20)–C(21)	1.391(4)	C(19)–C(20)–C(23)	121.4(2)
C(21)–C(22)	1.393(4)	C(21)–C(20)–C(23)	121.2(2)
C(17)–C(22)	1.401(4)	O(2)–C(24)–C(25)	123.9(2)
O(2)–C(24)	1.363(3)	O(2)–C(24)–C(29)	115.4(2)
C(24)–C(25)	1.399(4)	C(24)–C(25)–C(26)	119.1(3)
C(25)–C(26)	1.376(4)	C(25)–C(26)–C(27)	121.4(3)
C(26)–C(27)	1.397(4)	C(26)–C(27)–C(28)	118.8(3)
C(27)–C(28)	1.383(4)	C(27)–C(28)–C(29)	121.7(3)
C(28)–C(29)	1.387(4)	C(24)–C(29)–C(28)	118.3(3)
C(24)–C(29)	1.411(4)	C(25)–C(24)–C(29)	120.6(3)
		C(24)–C(25)–C(30)	120.6(3)
		C(26)–C(25)–C(30)	120.3(3)
		C(24)–C(29)–C(31)	119.5(3)
		C(28)–C(29)–C(31)	122.2(2)

[a] Estimated standard deviations are given in parentheses.

Ni–(Cp centroid) distance increases from 1.755 to 1.768 Å, the Ni–P distance increases from 2.1618(6) to 2.1696(8) Å, and the O–Ni–L (L = Cp centroid, PEt₃) angles expand from 125.4° and 92.99(5)° to 126.5° and 96.11(6)°, respectively. The slight lengthening of the Ni–O bond from 1.889(2) Å in **4** to 1.909(2) Å in **4·HOXyl** can also be understood in this context. Interestingly, the C(aryl)–O distance in the cresolate ligand lengthens from 1.330(3) to 1.350(3) Å, and the C(ring)– C(ipso)–C(ring) angle expands from 116.9(2)° to 117.4(2)°, indicating that delocalization of electrons from the electron-rich oxygen into the aromatic ring of the cresolate decreases upon coordination of the 2,6-dimethylphenol.[33]

When an excess of *p*-cresol was added to a C_6D_6 solution of thiocresolate **5** in an attempt to determine K_{eq}, the color of the solution changed from green-brown to red. It seemed possible that this behavior could be due to hydrogen bonding, because thiolate ligands have recently been shown to be weak hydrogen-bond acceptors.[39] However, NMR and UV/vis analysis showed that there was no new complex in solution; this behavior appears to be associated with the polarity of the solvent (red in more

(39) Kapteijn, G. M.; Grove, D. M.; Smeets, W. J. J.; Kooijman, J.; Spek, A. L.; van Koten, G. *Inorg. Chem.* **1996**, *35*, 534.

Table 3. Half-lives of the Phosphine Exchange Reaction in $C_6D_6{}^a$

X	T (°C)	approximate $t_{1/2}$
OTol	25	<2 min
NHTol	25	15 min
STol	45	6 h
CH₂Ph	75	1 d
Me	75	2 d
H	25	<5 min

^{a} Half-lives for equilibration of the reaction in eq 7 were based on monitoring the reaction by ^1H and $^{31}P\{^1H\}$ NMR spectroscopy.
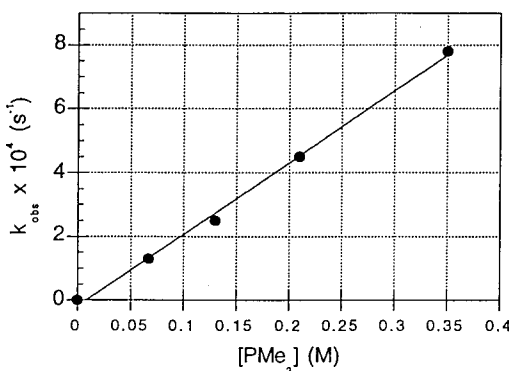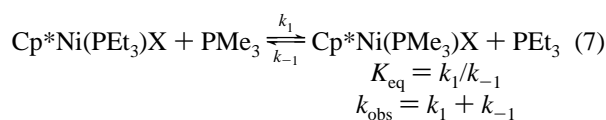

Figure 4. Concentration dependence of the pseudo-first-order rate constant for the reaction Cp*Ni(PEt₃)OTol + PMe₃ → Cp*Ni(PMe₃)-OTol + PEt₃ at 235 K.

polar solvents; green in nonpolar solvents) as well as the polarity of the thiolate group itself (*e.g.*, **5** is green in nonpolar solvents; **5-CF₃** is red under all conditions). This is reminiscent of color differences found in CpNi(PR′₃)SR complexes described some time ago.[40–42]

Exchange of Triethylphosphine with Trimethylphosphine. The lability of phosphine groups in the various Cp*Ni(PEt₃)X complexes vary drastically with the nature of X. Estimates of the half-lives of the reaction of Cp*Ni(PEt₃)X with PMe₃ (∼1 equiv) are given in Table 3. In each case, K_{eq} was estimated to be between 1 and 5, but in most cases this could not be measured accurately because of decomposition at long reaction times.

Kinetic studies of this reaction were pursued with X = OTol (**4**) and X = STol (**5**) in the presence of large excesses of PMe₃, in order to isolate the forward rate constant k_1. Repetition of

$$\text{Cp*Ni(PEt}_3\text{)X} + \text{PMe}_3 \underset{k_{-1}}{\overset{k_1}{\rightleftharpoons}} \text{Cp*Ni(PMe}_3\text{)X} + \text{PEt}_3 \quad (7)$$
$$K_{eq} = k_1/k_{-1}$$
$$k_{obs} = k_1 + k_{-1}$$

the experiment under such "flooding" conditions showed that the pseudo-first-order rate constants were linearly dependent on [PMe₃]. Graphs of k_{obs} vs PMe₃ concentration are shown in Figure 4 (X = OTol) and Figure 5 (X = STol). These data can be used to calculate rate constants of $k_{235K} = (2.2 \pm 0.1) \times 10^{-3}$ M⁻¹ s⁻¹ for **4** and $k_{305K} = (1.37 \pm 0.04) \times 10^{-4}$ M⁻¹ s⁻¹ for **5**; each rate law is of the type rate = k[Cp*Ni(PEt₃)X][PMe₃].

In order to examine the effect of an electron-withdrawing X group on the rate of this reaction, Cp*Ni(PEt₃)(p-SC₆H₄CF₃) (**5-F₃**) was synthesized. The rate constant for phosphine exchange ($k_{305K} = (1.40 \pm 0.05) \times 10^{-4}$ M⁻¹ s⁻¹) is the same as for its unsubstituted analogue, within experimental error
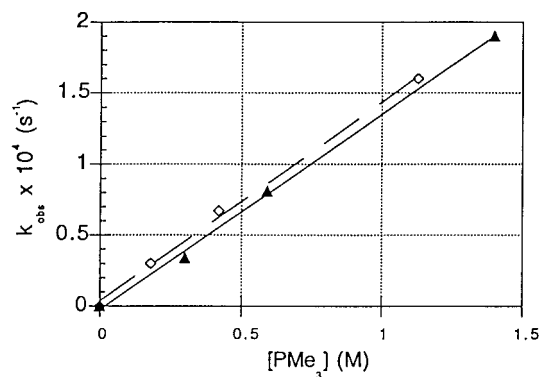
Figure 5. Concentration dependence of the pseudo-first-order rate constants for the reactions Cp*Ni(PEt₃)SAr + PMe₃ → Cp*Ni(PMe₃)-SAr + PEt₃ at 305 K. Dashed line, diamonds: Ar = p-Tol. Solid line, triangles: Ar = p-C₆H₅CF₃.

(Figure 5). Thus, an electron-withdrawing group in the aryl ring of **5** does not substantially affect the rate of phosphine exchange.

Discussion

Syntheses of New (Pentamethylcyclopentadienyl)nickel Complexes. Generation of a nickel triflato species from Cp*Ni-(PEt₃)Me[22] has made it possible to prepare unsupported amido and methoxo complexes of nickel(II). Each of these classes of compounds is rare. Very few monomeric amido complexes of group 10 transition metals were known until recently,[2,43,44] but a flurry of recent activity has centered around palladium amides.[14,45–50] Monomeric, unsupported nickel amides have been synthesized recently by the Hillhouse[10,51] and Boncella[11] groups; both groups utilized a square-planar nickel(II) core. The amido complexes reported here, like those of Boncella, are prone to ligand loss and dimerization.[7] In this case, dimerization to give [Cp*Ni(μ-NHR)]₂ could be avoided by using the triethylphosphine rather than the trimethylphosphine ligand; the PEt₃ adducts were isolable and stable for a reasonable amount of time in solution at room temperature. Attempts to synthesize analogous (alkylamido)nickel complexes were unsuccessful,[45] since the strong base deprotonated the Cp* ligand to give the nickel(0) complex **2**.

Late-metal methoxo complexes are even more rare, because β-hydride elimination can be a facile pathway for such compounds.[2,43] However, **3** is coordinatively and electronically saturated, disfavoring this pathway.[52,53] Although a few monomeric nickel methoxide complexes have been reported, their characterization would be considered incomplete by today's standards.[54–58] Complex **3**, on the other hand, has been fully

(40) Cooke, J.; Green, M.; Stone, F. G. A. *J. Chem. Soc., A* **1968**, 170.
(41) Davidson, J. L.; Sharp, D. W. A. *J. Chem. Soc., Dalton Trans.* **1972**, 107.
(42) Sato, M.; Yoshida, T. *J. Organomet. Chem.* **1972**, *39*, 389.

(43) Fryzuk, M. D.; Montgomery, C. D. *Coord. Chem. Rev.* **1989**, *95*, 1.
(44) Cowan, R. L.; Trogler, W. C. *J. Am. Chem. Soc.* **1989**, *111*, 4750.
(45) Villanueva, L. A.; Abboud, K. A.; Boncella, J. M. *Organometallics* **1994**, *13*, 3921.
(46) Driver, M. S.; Hartwig, J. F. *J. Am. Chem. Soc.* **1995**, *117*, 4708.
(47) Louie, J.; Paul, F.; Hartwig, J. F. *Organometallics* **1996**, *15*, 2796.
(48) Kim, Y.-J.; Choi, J.-C.; Osakada, K. *J. Organomet. Chem.* **1995**, *491*, 97.
(49) Widenhoefer, R. A.; Buchwald, S. L. *Organometallics* **1996**, *15*, 2755.
(50) Widenhoefer, R. A.; Buchwald, S. L. *Organometallics* **1995**, *14*, 3534.
(51) Matsunaga, P. T.; Hess, C. R.; Hillhouse, G. L. *J. Am. Chem. Soc.* **1994**, *116*, 3665.
(52) Hartwig, J. F. *J. Am. Chem. Soc.* **1996**, *118*, 7010.
(53) β-Hydrogen elimination can proceed through other pathways in coordinatively saturated complexes. See: Ritter, J. C. M.; Bergman, R. G. *J. Am. Chem. Soc.* **1997**, *119*, 2580.
(54) Birkenstock, U.; Bönnemann, H.; Bogdanovic, B.; Walter, D.; Wilke, G. *Adv. Chem. Ser.* **1968**, *70*, 250.

characterized, including X-ray crystallography; this is the first crystallographically characterized monomeric nickel methoxide compound.

Nickel hydrido complexes are important intermediates in organometallic[59−61] and biological processes,[62] but few such species have actually been isolated.[62−65] The easy isolation and characterization of **6** thus serves as an example of steric protection of this functionality. The very well-behaved crystal structure determination of **6** makes it possible to characterize the Ni−H bond length as 1.46(3) Å,[66] and the large range of other Cp*Ni(PEt₃)X structures allows us to characterize this as a distance characteristic of a coordination number between 4 and 6.[22]

Reactivity of an Unsupported Ni−N Bond. The nickel−nitrogen bond in **1a** reacts with polarized $X^{\delta -}-Y^{\delta +}$ bonds to place the more electronegative group on nickel and the less electronegative group on nitrogen. This is general for electronegative X in XH (X = OR, Osilica, NHR, SR), substrates with electropositive Y in YH (X = BR₂, SiR₃), organometallics, and trimethylsilyl chloride. Less polar bonds (H−H, C−H) do not react with **1a** faster than it decomposes.

The decomposition of **1a** takes place by deprotonation of another acid, the coordinated pentamethylcyclopentadiene ligand. The reducing ligand environment of phosphine and alkene undoubtedly favors the reduction of Ni(II) to Ni(0), as does the large effective concentration of an intramolecular C−H bond. Our group has previously observed decomposition of an amide complex by Cp* deprotonation;[67] interestingly, similar processes have been used to functionalize Cp* rings in other late transition metal systems.[68,69]

The reactivity of **1a** indicates that the Ni−N bond is strongly polarized, with an electrophilic nickel atom and a nucleophilic nitrogen atom. Although the X-ray crystal structure shows the presence of a covalent Ni−N bond, it is possible that **1a** in solution is in equilibrium with an ionic tautomer through which it reacts. Recently, the reactivity of a ruthenium hydroxide has been rationalized by invoking such a pathway.[5]
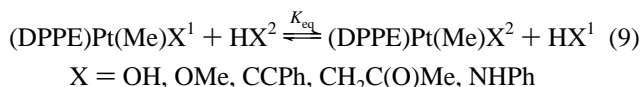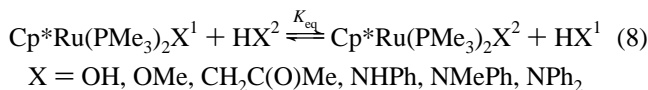
The presence of *free* ions in either of these reactions seems unlikely, because the reactions proceed rapidly in nonpolar solvents such as benzene and pentane, in which formation of free ions is difficult.[70] In the case of **1a**, we have also made the following observations that are inconsistent with the presence of free amide anions: (a) no reaction is observed with esters or carboxamides, and (b) the bulky weak acids *tert*-butyl alcohol and diphenylamine are also inert to **1a**. However, the presence or absence of ion pairs (either contact or solvent-separated) is more difficult to establish. It seems reasonable that decomposition of **1a** to **2** is mediated by an ion pair; this is consistent with the higher solution stability of the phenolate and thiophenolate analogues **4** and **5**, in which X is less basic.

Another way to rule out the presence of free or solvent-separated ion pairs is to confirm that the "anion" does not exchange between metals in solution. Recent kinetic studies on rhenium alkoxide compounds used a double-labeling experiment to show that alkoxide groups do not exchange between metal centers.[37,71] Literature kinetic and conductance evidence also argues against the dissociation of late transition metal−N and −O bonds into free ions in nonpolar solvents.[2,4] However, the polarization of this bond gives rise to substantial reactivity. The extremely strong hydrogen bond formed between **4** and phenols, as well as the metrical changes between **4** and **4-HOXyl** discussed above, are also a testament to the amount of electron density localized on the X atom in the ground state of aryloxonickel complexes.

Thermochemistry *via* Exchange Reactions. The equilibria observed between **1** and cresol, methanol, and other arylamides provide information about relative Ni−O and Ni−N bond energies in the Cp*Ni(PEt₃)X system.

The use of exchange reactions to derive the relative bond dissociation energies of late metal−ligand bonds has been employed most extensively in work by Bryndza and Bercaw.[72] In this work, the series of equilibria in eqs 8 and 9 were evaluated. Assuming that replacement of X^1 with X^2 does not

$$\text{Cp*Ru(PMe}_3)_2\text{X}^1 + \text{HX}^2 \overset{K_{eq}}{\rightleftharpoons} \text{Cp*Ru(PMe}_3)_2\text{X}^2 + \text{HX}^1 \quad (8)$$
$$\text{X = OH, OMe, CH}_2\text{C(O)Me, NHPh, NMePh, NPh}_2$$

$$\text{(DPPE)Pt(Me)X}^1 + \text{HX}^2 \overset{K_{eq}}{\rightleftharpoons} \text{(DPPE)Pt(Me)X}^2 + \text{HX}^1 \quad (9)$$
$$\text{X = OH, OMe, CCPh, CH}_2\text{C(O)Me, NHPh}$$

perturb the bond strengths within [M], X^1, or $X^{2,73,74}$ and assuming that ΔS for the reaction is zero,[75] the values of BDE-(H−X^1), BDE(H−X^2), and K_{eq} can be used to derive the difference between the M−X^1 and M−X^2 bond strengths. By finding K_{eq} for a large series of X ligands for which the H−X bond energies are known, a scale of relative M−X bond energies can be devised.

(55) Griffith, W. P.; Lewis, J.; Wilkinson, G. *J. Chem. Soc.* **1959**, 1775.

(56) Griffith, W. P.; Lewis, J.; Wilkinson, G. *J. Chem. Soc.* **1961**, 775.

(57) Feltham, R. D. *Inorg. Chem.* **1964**, *3*, 116.

(58) Bhaduri, S.; Johnson, B. F. G.; Matheson, T. W. *J. Chem. Soc., Dalton Trans.* **1977**, 561.

(59) Emad, A.; Rausch, M. D. *J. Organomet. Chem.* **1980**, *191*, 313.

(60) Müller, U.; Keim, W.; Krüger, C.; Betz, P. *Angew. Chem., Int. Ed. Engl.* **1989**, *28*, 1011.

(61) Seligson, A. L.; Cowan, R. L.; Trogler, W. C. *Inorg. Chem.* **1991**, *30*, 3371.

(62) James, T. L.; Cai, L.; Muetterties, M. C.; Holm, R. H. *Inorg. Chem.* **1996**, *35*, 4148 and references therein.

(63) Srivastava, S. C.; Bigorgne, B. *J. Organomet. Chem.* **1969**, *18*, P30.

(64) Saito, T.; Nakajima, M.; Kobayashi, A.; Sasaki, Y. *J. Chem. Soc., Dalton Trans.* **1978**, 482.

(65) Darensbourg, M. Y.; Ludwig, M.; Riordan, C. G. *Inorg. Chem.* **1989**, *28*, 1630.

(66) Note that bonds to hydrogen derived from X-ray crystallography are systematically short: Stout, G. H.; Jensen, L. H. *X-Ray Structure Determination: A Practical Guide*, 2nd ed.; Wiley: New York, 1989.

(67) Glueck, D. S.; Bergman, R. G. *Organometallics* **1990**, *9*, 2862.

(68) Wei, C.; Aigbirhio, F.; Adams, H.; Bailey, N. A.; Hempstead, P. D.; Maitlis, P. M. *Chem. Comm.* **1991**, 883.

(69) Gloaguen, B.; Astruc, D. *J. Am. Chem. Soc.* **1990**, *112*, 4607.

(70) An outer-sphere phenolate has been observed in a ruthenium complex, but this was aided by extensive hydrogen bonding to excess phenol. Burn, M. J.; Fickes, M. G.; Hollander, F. J.; Bergman, R. G. *Organometallics* **1995**, *14*, 137.

(71) Unfortunately, we have not been able to isolate pure samples of ethyltetramethylcyclopentadienyl analogues of the nickel amido complexes in order to perform crossover experiments here.

(72) Bryndza, H. E.; Fong, L. K.; Paciello, R. A.; Tam, W.; Bercaw, J. E. *J. Am. Chem. Soc.* **1987**, *109*, 1444.

(73) Benson, S. W.; Buss, J. H. *J. Chem. Phys.* **1958**, *29*, 546.

(74) This assumption has been questioned subsequently by Bryndza and Bercaw: Bryndza, H. E.; Domaille, P. J.; Paciello, R. A.; Bercaw, J. E. *Organometallics* **1989**, *8*, 379. They found that changing X in Cp*Ru-(PMe₃)₂X changed the barrier for phosphine exchange by >10 kcal/mol (since exchange proceeded through a dissociative mechanism, one can estimate $\Delta H^{\ddagger}_{exchange}$ = BDE_{Ru−P}), with N and O ligands giving the weakest Ru−P bond and C and H ligands giving the strongest Ru−P bond. In the system described here, the Ni−P bond lengths imply a similar trend (see ref 22). However, their phosphine dissociation was aided by π-bonding in the unsaturated intermediate; no such mechanism is possible for the complexes here (see ref 7). Since we have no way to accurately evaluate the Ni−P bond strengths, this effect is ignored here. Note that this does *not* invalidate our estimates of bond energy differences, because bond energies are defined to include changes in ancillary bonding (see footnote 34 in ref 87).

(75) Since translational entropy is conserved, ΔS should be small in systems in which two particles are converted into two particles. See: Minas de Piedade, M. E.; Simões, J. A. M. *J. Organomet. Chem.* **1996**, *518*, 167. Entropic factors in our system will be discussed more thoroughly below.

Figure 6. Hammett plot comparing log K_{eq} for the exchange in eq 1 to Hammett σ_p^-; $\rho = 3.4$.

Figure 7. Plot of relative Ni−N bond energy versus H−N bond energy;[78] slope = 1.9. Relative Ni−N bond energies were calculated as RT ln K_{eq} + BDE (H−N) − 92.0.[80]

In the study of Bryndza and Bercaw, the equilibrium constants for the reactions in eqs 8 and 9 were found to be near unity for exchanges between carbon (CCPh, $CH_2C(O)Me$), nitrogen (NHPh, NMePh), and oxygen (OH, OMe) ligands.[76] Thus, given the assumptions stated above, the bond dissociation of the M−X bond scales 1:1 with the bond dissociation of the H−X bond for these examples, as a graph of H−X bond energy vs M−X bond energy has a slope of one.[77,78] Since the H−X bond energies for these X groups span 50 kcal/mol, this was taken as an indication that this correlation is general over that large range of energies. This correlation implied a model for bonds between late transition metals and anionic ligands in which metal fragments bind in the same way as protons, and thus the late metal auxiliaries "behave like large hydrogens".[2] We will refer to this model as the "1:1 model", and once again note its important aspects: (a) a good correlation between $D(H−X)$ and $D(M−X)$, and (b) these quantities scale 1:1. In the data presented here, a *systematic* deviation from the 1:1 model is observed for the exchange of para-substituted arylamines for arylamido complexes of nickel. In this study, *electron-withdrawing amines favored nickel binding, and electron-donating amines favored proton binding.* The best correlation with Hammett or Taft parameters was found for σ_p^-, and this correlation held for para substituents from NMe_2 ($\sigma_p^- = -0.32$) to Ac ($\sigma_p^- = +0.87$).[79] The Hammett correlation is shown in Figure 6; $\rho = 3.4$. Thus, the formation of a nickel amide from an aniline is controlled by the same effects that control the deprotonation of phenols (the standard reaction used for defining σ^- parameters). These results cannot be explained in the context of the 1:1 model: in that model, electronic differences of the

ligand should affect H−X and M−X bonds equally, and the equilibrium constant should still be unity. This may also be stated as a relationship between BDE(H−NHAr)[80] and the BDE-(Ni−NHAr) that can be derived from these numbers, the K_{eq} values, and the entropy and group additivity assumptions discussed above. A diagram of our data in the style of ref 72 is shown in Figure 7. There is a reasonable correlation between H−X and M−X bond energies, but instead of a slope of unity, the slope is 1.9. Although our analysis was necessarily done over a smaller H−X BDE range, this is as large a range possible within a series of ligands with such similar substituents.

The exchange between the amide ligand in **1a** and the cresolate ligand in **4** (eq 4) shows another equilibrium constant that is unexpectedly large; this corresponds to $\Delta G°_{THF} = 6.0 \pm 0.3$ kcal/mol and $\Delta G°_{benzene} = 7.5 \pm 0.8$ kcal/mol. We were interested in determining whether this could be due to a large entropic effect. In the study of the Pt and Ru systems,[72] very different HX acids were used, and the entropic contribution was very small (in the absence of steric effects); it would be surprising if isosteric and electronically similar HX exchanges like the ones discussed here caused larger entropic changes. Unfortunately, limitations imposed by signal/noise ratios, solubility of the amine, and the thermal sensitivity of **1a** made it impossible to accurately gauge $\Delta S°$ for this reaction from the temperature dependence of the equilibrium constant. An independent assessment of $\Delta H(303 \text{ K}) = -9.4 \pm 0.2$ kcal/mol for eq 4 using solution calorimetry in benzene, however, confirmed that the large equilibrium constant is purely enthalpic. Thus, both calorimetric methods and equilibrium methods indicate strongly that the relative bond energies are not in accordance with the 1:1 model. Importantly, this substantial deviation was found not for a reaction with drastic differences between the X ligands, but for one where the steric and electronic properties of the organic fragment were carefully chosen to be the same.

We believe that the inequivalence of the equilibrium and calorimetric values of ΔH(benzene) is due to hydrogen bonding between **4** and HOTol in the mixture produced in the equilibration experiments. When a double equilibrium made up of eq 4 and an equilibrium representing formation of **4·HOTol** was mathematically modeled, the results confirmed that hydrogen

(76) The deviation of one example (NPh_2) was shown to be largely due to a steric (entropic) effect. Large deviations were also observed for X ligands that bind through a second-row atom or can participate in backbonding.

(77) The 1:1 correlation has sometimes been generalized to BDE(M-N) < BDE(M-O). This should only follow if BDE(H-N) < BDE(H-O), which, although true much of the time, is far from universal (*e.g.*, $H_2N−H = 107$ kcal/mol; PhO−H = 87 kcal/mol). Thus, such generalizations *must* be qualified. However, the present work shows that there is some truth to the generalization that BDE(M-NHR) < BDE(M-OR), because in this study, with L_nM and R (and, fortuitously, H−X BDE) held constant, the oxygen ligand binds more strongly than the nitrogen ligand.

(78) In this kind of graph, deviations from 1:1 behavior are dampened by the fact that *both* axes contain BDE(H-X). Thus, a systematic deviation from 1:1 behavior (such as that in ref 81) can appear to give a H−X/M−X graph with a slope nearly equal to 1.0.

(79) log (K_{eq}) had a poorer correlation with σ_p, because $\sigma_p(CF_3) > \sigma_p(Ac)$. Thus, the deprotonation of benzoic acids is a poorer model for Ni−N/H−N exchange, as are other Hammett substituent constants.
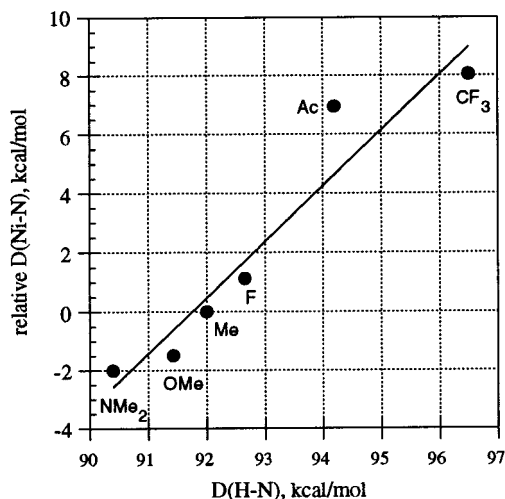
(80) ArNH−H bond energies in DMSO solution are given in: Bordwell, F. G.; Zhang, X.-M.; Cheng, J.-P. *J. Org. Chem.* **1993**, *58*, 6410. Some of the BDE values used here were extrapolated from the correlations between σ^- and the N−H bond energies found there.

bonding with a reasonable strength of 5−6 kcal/mol would cause the apparent equilibrium constant to vary from the actual equilibrium constant for eq 4 (as deduced from the calorimetrically determined ΔH value and the assumption that $\Delta S \approx 0$) by the amount observed.

A New Model for Thermochemistry and Reactivity. Deviations from the 1:1 correlation between BDE(H−X) and BDE(M−X) are not unique to this nickel auxiliary. A series of para-substituted phenoxorhenium complexes have been exchanged with the corresponding phenols by the Mayer group; as here, electron-withdrawing groups stabilized the M−O bond relative to the H−O bond.[81] Their equilibrium constants correlated well with Hammett σ ($\rho = 0.71$), although fewer very electron-deficient substituents were used in comparison with our study. At that time, the O−H bond energies for these phenols were not known, but a plot of BDE (H−O) vs BDE (Re−O) using recently published solution O−H bond energy data gives a straight line with a slope of 1.07.[78,82] Thus, a systematic deviation from the 1:1 model, albeit a smaller deviation, is observed with a third-row metal and oxygen rather than nitrogen ligands. In other late-metal systems, exchanges of platinum glycolate complexes,[83] phenolatoiridium complexes,[34] and rhenium amido complexes[84] have electronic effects similar to those observed in this nickel system. However, the only complexes that have systematically incorporated a large number of substituents with little steric change, besides the rhenium alkoxides discussed above, are the arylrhodium complexes Cp*Rh(PMe$_3$)(Ar)(H) (Ar = 3,5-C$_6$H$_3$X$_2$), a series for which the corresponding C−H bond energies are not known.[85] As a result, a similar plot for these exchanges cannot be constructed, but it is evident that a distinct preference for electron-withdrawing X on the metal is present, consistent with a deviation from the 1:1 model like the one in the nickel system.

The exchange of **1a** and methanol with **3** and amine was the only exchange in which the prediction of the 1:1 model was upheld; the equilibrium constant of 0.1 for eq 3 is only an order of magnitude different from the K_{eq} of 2.3 for the analogous exchange with Cp*Ru(PMe$_3$)$_2$X compounds.[72] However, the ruthenium study did not include the OTol ligand; it included *alk*oxide and *aryl*amide ligands, but no examples of aryloxide or alkylamide complexes for a more systematic comparison. In the nickel system, **1a** or **3** was completely converted to **4** to within our detection limits when 1 equiv of cresol was added. This deviation cannot be explained by the large difference in dissociation energy between the MeO−H bond (104 kcal/mol) and the ArO-H bond (~87 kcal/mol)[86] because, according to the 1:1 model, this should be compensated by a much larger Ni-OMe than Ni-OAr bond strength.

In order to compare the large equilibrium constant for NHTol/ OTol exchange at nickel to the (DPPE)Pt(Me)X system for which the 1:1 model was demonstrated, we have investigated an analogous exchange at Pt. Through ^{1}H NMR analyses like those used for the nickel experiments, we have found that the equilibrium constant with X^1 = TolO and X^2 = TolNH in eq 9 is approximately 4×10^{-4}. As above, this deviation from the 1:1 model cannot be caused by hydrogen bonding, because

hydrogen bonding acts to make the apparent equilibrium constant closer to one than the true equilibrium constant. Thus, a metal fragment for which the 1:1 model was previously believed to hold is not immune to the thermodynamic preference for oxygen found here.

The literature also substantiates the preference for isosteric oxygen over nitrogen ligands, relative to their H−X counterparts. For example, phenols displace arylamides and alkoxides quantitatively in other series of complexes.[37,87,88] Some early metal systems also follow these trends. When aryl ligands are exchanged in an ingeniously devised chelating scandium system, the carbon atom of the aryl ring with the *para*-CF$_3$ substituent binds preferentially.[89] The bond energy orders in early metal systems studied by Marks show that M−O bonds are disproportionately (relative to a 1:1 correlation) strong with respect to M−N bonds.[90] Also, density functional calculations predict that $(D([M]-OH) - D(H-OH)) - (D([M]-NH_2) - D(H-NH_2)) = 9$ kcal/mol for [M] = (CO)$_4$Co *and* Cl$_3$Ti.[91] Taken together, these results suggest that some factor causes a preference for oxygen over nitrogen ligands in metal binding for *both* early and late transition metals; this will be addressed more fully below.

We have shown that the 1:1 model does not hold when only the heteroatom is changed in isosteric ligands or when the para substituent in an arylamido ligand is varied. Thus, we sought a model in which σ or π effects cause transition metals to favor aryl substituents over alkyl substituents, oxygen over nitrogen, and electron-withdrawing substituents over electron-donating ones, relative to hydrogen.

A tempting explanation for the deviation found from the 1:1 H-X/M-X BDE model lies in repulsive nonbonded interactions between filled d orbitals on the nickel atom and the p orbital(s) on the X atom.[92] Nitrogen is a stronger π donor than oxygen, both in organic and organometallic[93,94] systems, so amido complexes would be destabilized relative to aryloxo complexes, as observed. More extensive delocalization of the electrons in the nitrogen p-orbital into the aryl ring in the electron-withdrawing amides would explain the K_{eq} values for amido/ amine exchange (eq 1). However, several observations are inconsistent with this explanation. First, the exchange in eq 1 was repeated using *m*-(dimethylamino)aniline; for this reaction, $K_{eq} = 1.1 \pm 0.2$. The small difference between the equilibrium constants found with a *m*-dimethylamino substituent (strongly electron-withdrawing) and a *p*-dimethylamino substituent (strongly electron-donating) suggests that resonance effects do not play a dominant role. In addition, the geometry of **1a** (as shown in the crystal structure and discussed above) is such that pπ−dπ repulsion is minimized by steric forces. Finally, the good Hammett correlation with σ_p^- implies that Ni−NHAr/H−NHAr exchange is affected by the same factors as Na−OAr/H−OAr exchange (the standard for σ_p^- parameters), *i.e.*, the interaction

(81) Erikson, T. K. G.; Bryan, J. C.; Mayer, J. M. *Organometallics* **1988**, *7*, 1930.

(82) ArO−H bond energies in DMSO solution are given in: Bordwell, F. G.; Cheng, J.-P. *J. Am. Chem. Soc.* **1991**, *113*, 1736.

(83) Andrews, M. A.; Voss, E. J.; Gould, G. L.; Klooster, W. T.; Koetzle, T. F. *J. Am. Chem. Soc.* **1994**, *116*, 5730.

(84) Simpson, R. D.; Bergman, R. G. *Organometallics* **1992**, *11*, 4306.

(85) Selmeczy, A. D.; Jones, W. D.; Osman, R.; Perutz, R. N. *Organometallics* **1995**, *14*, 5677.

(86) Gas-phase BDEs: McMillen, D. F.; Golden, D. M. *Annu. Rev. Phys. Chem.* **1982**, *33*, 493.

(87) Hartwig, J. F.; Andersen, R. A.; Bergman, R. G. *Organometallics* **1991**, *10*, 1875.

(88) Glueck, D. S.; Winslow, L. J. N.; Bergman, R. G. *Organometallics* **1991**, *10*, 1462.

(89) Bulls, A. R.; Bercaw, J. E.; Manriquez, J. M.; Thompson, M. E. *Polyhedron* **1988**, *7*, 1409.

(90) Schock, L. E.; Marks, T. J. *J. Am. Chem. Soc.* **1988**, *110*, 7701. A reviewer has pointed out that these bond energies are undoubtedly affected by constructive π-interaction between M and X.

(91) Ziegler, T.; Tschinke, V.; Versluis, L.; Baerends, E. J.; Ravenek, W. *Polyhedron* **1988**, *7*, 1625. Although absolute bond energies derived from calculations are usually not highly accurate, *differences* in bond energies are more trustworthy.

(92) Caulton, K. G. *New J. Chem.* **1994**, *18*, 25.

(93) Darensbourg, D. J.; Klausmeyer, K. K.; Reibenspies, J. H. *Inorg. Chem.* **1996**, *35*, 1529; 1535.

(94) Espinet, P.; Bailey, P. M.; Maitlis, P. M. *J. Chem. Soc., Dalton Trans.* **1979**, 1542.

between Ni and N in complexes **1** is mostly σ in character like the interaction between Na and O in NaOAr. Thus, a pπ−dπ repulsion model may not be the best explanation for our data.

Instead, we propose that the ground-state energy differences in these nickel complexes are associated with substantial charge polarization in the late M−X bond. This polarization simply corresponds to the significant electronegativity difference between transition metals and N or O and is not primarily π in character. A similar model based on electronegativities has been advanced to explain bond energy correlations in early transition metal and lanthanide complexes.[95] In this qualitative model, factors that stabilize the partial negative charge on the N or O atom will stabilize the metal complex. Thus, in the energies of metal complexes relative to their H−X analogues, the more electronegative oxygen will be favored over nitrogen, delocalizing aryl groups will be favored over alkyl groups, and electron-withdrawing substituents will be favored.

The fact that metal complexes are more stable with a more stable anion presumably reflects a large component of electrostatic bonding in metal−X bonds. This is conveniently described using the $E−C$ model of Drago,[96] in which one would state that the transition metal has a greater inclination to bind electrostatically than covalently to an anionic ligand. A $\Delta E^X − \Delta C^X$ substituent constant analysis of log (K_{eq}) for the nickel amido/amine exchanges described above (eq 1) gave sensitivity factors of $d^E = -18.4$ and $d^C = 1.84$ ($R^2 = 0.985$).[97] Although the linear regression analysis used only the six points for the para substituents, the substituents varied widely in their $\Delta C^X/\Delta E^X$ ratios, so the ratio $d^C/d^E = -0.1$ indicates that electrostatic factors play a much larger role in determining the bond energy difference than covalent factors.[98] However, as argued above, this does not necessarily imply that the Ni−N bond is ionic or that full heterolysis of this bond occurs during the reactions of complexes **1**. The signs of d^E and d^C also demonstrate that electrostatically, electron-withdrawing groups favor stronger Ni−N than H−N bonds, but covalently, electron-donating groups favor stronger Ni−N than H−N bonds. In this nickel system, electrostatic effects dominate and so a preference for electron-withdrawing groups on nickel is observed overall.

Importantly, the electrostatic character of the Ni−N bond found in this model is consistent with the reactivity of **1a** toward polarized bonds, and the large amount of Ni⁺ OTol⁻ character in the crystal structure of **4** discussed above. Thus, a simple model (based ultimately on the ideas of Pauling) can explain both the ground-state and reactivity properties of this class of molecules.

We do not wish to suggest that destabilizing nonbonding π interactions between metals and nitrogen or oxygen lone pairs do not exist. However, the evidence above suggests that this force is not the major one responsible for the preference of oxygen over nitrogen ligands, at least in this system. Further, in view of the success with which the electrostatic model

(95) Marks, T. J.; Gagne, M. R.; Nolan, S. P.; Schock, L. E.; Seyam, A. M.; Stern, D. *Pure Appl. Chem.* **1989**, *61*, 1665.

(96) (a) Drago, R. S. *Applications of Electrostatic-Covalent Models in Chemistry*; Surfside: Gainesville, FL, 1994. Drago's theory only applies to *enthalpy* changes; the same zero-entropy assumptions applied above must be made to apply an $E−C$ analysis to our system. Note tht the analysis here reflects Drago's T and R terms, which undoubtedly are incorporated into our d_E because they contribute to ionicity. A more complete analysis of M−X energies (and a similar criticism of the 1:1 model) in the context of *ECT* theory may be found in: (b) Drago, R. S.; Wong, N. M.; Ferris, D. C. *J. Am. Chem. Soc.* **1992**, *114*, 91.

(97) Drago, R. S. *Inorg. Chem.* **1995**, *34*, 3543. This gives a result that is the two-dimensional analogue of a Hammett correlation; instead of a ρ value, one obtains d^C (the sensitivity to covalent factors) and d^E (the sensitivity to electrostatic factors).

(98) The d^C/d^E ratio also accounts for the good fit found with σ_p^- ($d^C/d^E = -0.05$) but not with σ ($d^C/d^E = +0.10$).

Scheme 4
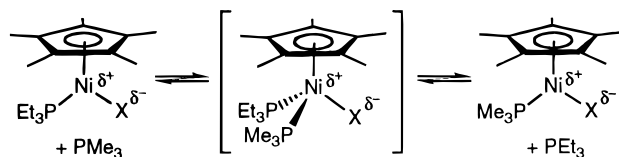
advanced above replaces the need for the pπ−dπ model, one might suggest that many of the phenomena ascribed to non-bonded pπ−dπ repulsions simply reflect the electrostatic component of M−X bonds.[92,99] When polarization effects can explain the data, "Ockham's razor" dictates that there is no reason to add additional variables (here, π-symmetry repulsion) to the model. Thus, the simple $E−C$ model presented here can rationalize thermochemical data for saturated complexes with no need to postulate additional forces. For *unsaturated* complexes, though, metal−ligand π interactions clearly affect the bonding substantially, as shown by many workers.[92] Indeed, in a recent example of systematic alkoxide exchanges at an unsaturated vanadium center, a stability order *opposite* to ours was found.[100]

Phosphine Exchange Rates Also Reflect Ni−X Polarization. The triethylphosphine ligand also takes part in exchange reactions (Scheme 4), and the rates depend on the nature of X. In the series with isosteric X ligands the rate trend is OTol > NHTol > STol > CH₂Ph; the nickel atoms with the most electronegative X ligands exchange phosphine ligands the most rapidly. This order does *not* correspond to π-donation ability (NHTol > OTol), a trend that has been observed for exchanges of phosphine ligands in 18-electron phosphine complexes.[74,92] In several cases, the nickel complexes were sufficiently stable to excess PMe₃ that flooding experiments could be used to determine the overall rate law. With X = OTol (**4**) or SAr (**5, 5-F₃**), the reaction had a first-order dependence on both [Cp*Ni-(PEt₃)X] and [PMe₃], indicating that the incoming phosphine is coordinated to the metal in the rate-determining transition state. Scheme 4 shows a reasonable mechanism that involves a 20-electron Cp*NiL₂X intermediate; this mechanism is consistent with the second-order rate law and the high rate for phosphine exchange in the case of the extremely small hydride ligand. Although this intermediate violates the "18-electron rule," an isolable Cp*NiXL₂ complex, Cp*Ni(η^2-acac)(PEt₃), has recently been crystallographically characterized, demonstrating that nickel complexes similar to this intermediate are accessible.[32,101]

The rates of phosphine substitution are consistent with the polarized Ni−X model presented above. Thus the nickel cresolate, which has the most electrophilic nickel atom, reacts most rapidly, and the nickel alkyl complexes, which have less electrophilic Ni atoms, react most slowly. In an attempt to substantiate the electrostatic explanation for the rate ordering, the rate of the phosphine exchange for the electron-withdrawing thiolate **5-F₃** was measured. The rate constant was equivalent to that for the *p*-methyl-substituted thiolate, showing that this variation did *not* affect the rate! One can tentatively explain

(99) Mayer, J. M. *Comments Inorg. Chem.* **1988**, *8*, 125.

(100) Thorn, D. L.; Harlow, R. L.; Herron, N. *Inorg. Chem.* **1996**, *35*, 547.

(101) Two referees have questioned the necessity of a 20-electron intermediate, instead favoring intermediates with loose ionic bonding (*i.e.*, [Cp*Ni(PEt₃)(PMe₃)]⁺···[X]⁻) or a slipped Cp ring. Although we cannot rule out either intermediate on the basis of our data, the conclusive characterization of Cp*Ni(η^2-acac)(PEt₃) as a three-legged piano stool with a symmetric, η^5-Cp in ref 32 (as well as the more stereotypical example, nickelocene, which has two symmetric η^5-Cp rings) leads us to believe that a simple associative mechanism is quite reasonable, the 18-electron "rule" (for which there are many exceptions) notwithstanding.

12810   *J. Am. Chem. Soc., Vol. 119, No. 52, 1997*

Holland et al.

this result by postulating that the Ni−S bond has much less electrostatic character than the Ni−N and Ni−O bonds, and is thus less susceptible to electronic changes in the ligand. This suspicion was supported by the small para-substituent dependence of the equilibrium constant for protic exchange of thiolate ligands (eq 6).

It was not feasible to examine the rate laws of the M−X/ H−X′ exchanges (eqs 1 and 4) above because of thermal instability, detection limits, and rapid rates. However, the mechanism of the phosphine exchange reactions may be used to speculate on the mechanism of proton exchange. First, an incoming HX′ compound could form a transient hydrogen bond between its proton and the nucleophilic nickel-bound X atom (as in **4·HOAr**). This could be accompanied by coordination of X′ to the nickel atom; coordination is well-known to lower the pK_a of α-hydrogen atoms. Our mechanistic study of phosphine exchange indicates that a coordination site is available, resulting in a symmetric intermediate, analogous to that in Figure 2, that can break either H−X bond to either revert to starting materials or continue to product. This "σ-bond metathesis" mechanism is analogous to those proposed for exchanges of alkoxide ligands at rhenium.[37,81]
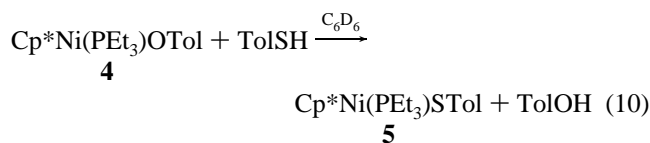
Conclusions: Generality of a Qualitative *E−C* Model. The 1:1 model is a qualitatively correct model that is useful for estimating relative M−X bond energies, particularly when the H−X bond dissociation energies span a wide range. However, deviations from this generalization exist when H-X bond energies are varied systematically over a small range by the use of very similar ligands. Thus, the arguments presented here indicate that the 1:1 model, in which the proton and the transition metal bind to X with similar covalent vs electrostatic contributions, should be amended to incorporate more electrostatic contribution in metal−N and metal−O bonds than in H−N and H−O bonds.

The electrostatic modification to the 1:1 model may be general to all bonds between electronically saturated metals and anionic ligands, to differing degrees. In a series of exchanges at rhenium, a similar preference for electron-withdrawing X, though muted, is observed.[81] Because the electronegativity of the third-row metal is not much lower than that of hydrogen, the electrostatic bonding tendency does not differ as much between a proton and the transition metal. In another series of exchanges, platinum was shown to favor more electron-*donating* alkoxides relative to sodium alkoxides.[102] Thus, consistent with our model, when presented with a choice between a more electrostatically binding metal center, Na(I), and a less electrostatically binding metal, Pt(II), electron-withdrawing groups favor the former and electron-donating groups the latter. These qualitative arguments follow the *E−C* model of Drago, which can also be used quantitatively.[103] The addition of π-symmetry repulsive effects to the model is not necessary to qualitatively explain the data in these electronically saturated complexes, although π effects may eventually be evaluated from deviations from a quantitative *E-C* model.[96]

Although exchanges of M−X and H−X (X = anionic ligand) favor electron-*withdrawing* groups on the metal, exchanges of neutral ligands (L) favor electron *donating* groups bound to M, in metal complexes of arene ligands,[104] olefin ligands[105−109] and

phosphine ligands.[110,111] This reflects a switch from more electrostatic bonding in M−X to more covalent bonding in M−L, and is reflected in the large C_B/E_B ratios found for phosphine ligands.[112] In the terms of an *E−C* model, this means that transition metals also have a substantial ability to bind covalently when the ligand is not receptive toward electrostatic bonding. In the *E−C* analysis of the nickel amido/amine exchanges above, the covalent terms *did* favor electron-*donating* groups, even though this was obscured by the larger electrostatic effect. Thus, in a qualitative sense, this verifies that *E* and *C* parameters can be used to understand the two completely different series of bond strength trends.

The high stability of thiolate complexes can also be explained in terms of a qualitative *E−C* model. When aryl thiols were added to **1a** or **4**, there was complete, irreversible conversion to the thiolate complex **5**. The values of Δ*H* for these reactions

$$\text{Cp*Ni(PEt}_3\text{)OTol} + \text{TolSH} \xrightarrow{\text{C}_6\text{D}_6}$$
$$\mathbf{4}$$

$$\text{Cp*Ni(PEt}_3\text{)STol} + \text{TolOH} \quad (10)$$
$$\mathbf{5}$$

were found to be −23.0 kcal/mol and −14.0 kcal/mol, respectively. This preference for a second-row main-group element, consistent with results by Bryndza[72] and Glueck[113] for the (DPPE)Pt(Me)X system, has generally been attributed to soft/ soft effects. A similar argument, using a qualitative *E−C* model, can rationalize these observations equally well. Bonds from *second*-row elements to metals should have a larger contribution from covalent bonding (C_B), independent of the electrostatic trend.[96] In this case, the covalent trend (favoring electron-donating substituents) should be able to compete more effectively with the electrostatic trend (favoring electron-withdrawing substituents); this is indeed observed in the lower sensitivity of thiol/thiolate equilibria to substituent variation (eq 6). In another result suggesting the separation of *E* (favoring more electronegative ligating atoms) and *C* (favoring second-row over first-row ligating atoms) variables, the (DPPE)Pt(Me)X system prefers thiolate over phosphide ligands, and both of these are preferred over C, N and O ligands.[113] Hopefully, future work will elaborate the range of applicability of this qualitative *E−C* model in the chemistry of M−X complexes of the late transition metals.

Experimental Section

General. All manipulations were carried out in oven-dried glassware either using standard Schlenk techniques or in a Vacuum Atmospheres circulating inert atmosphere glove box. Celite and silica were dried overnight at 200 °C under dynamic vacuum. Pentane, diethyl ether, hexanes, hexamethyldisiloxane, toluene, C_6H_6, C_6D_6, THF, and THF-d_8 were dried over Na/benzophenone. Methylene chloride and CD_2-Cl_2 were dried over calcium hydride. Methanol was distilled from

(102) Dockter, D. W.; Fanwick, P. E.; Kubiak, C. P. *J. Am. Chem. Soc.* **1996**, *118*, 4846.

(103) See ref 96. We hope that others will carry out quantitative *E−C* analyses that test the generality of the notions presented here. Such studies should be performed on more robust systems than these nickel complexes, so that entropy changes can be evaluated, and so that decomposition does not limit the choice of ligands.

(104) Nolan, S. P.; Martin, K. L.; Stevens, E. D.; Fagan, P. J. *Organometallics* **1992**, *11*, 3947.

(105) Doherty, N. M.; Bercaw, J. E. *J. Am. Chem. Soc.* **1985**, *107*, 2670.

(106) Kurosawa, H.; Ikeda, I. *J. Organomet. Chem.* **1992**, *428*, 289.

(107) Kurosawa, H.; Miki, K.; Kasai, N.; Ikeda, I. *Organometallics* **1991**, *10*, 1607.

(108) Rix, F. C.; Brookhart, M.; White, P. S. *J. Am. Chem. Soc.* **1996**, *118*, 2436.

(109) Burger, B. J.; Santarsiero, B. D.; Trimmer, M. S.; Bercaw, J. E. *J. Am. Chem. Soc.* **1988**, *110*, 3134.

(110) Luo, L.; Li, C. B.; Cucullu, M. E.; Nolan, S. P. *Organometallics* **1995**, *14*, 1333.

(111) The opposite order can be observed when back-bonding is important, as in pyridines: Kulig, J.; Lenarcik, B.; Rzepka, M. *Pol. J. Chem.* **1987**, *61*, 735. However, more recently, it was found that electron-donating substituents cause stronger pyridine binding in B₁₂ models: Garr, C. D.; Sirovatka, J. M.; Finke, R. G. *Inorg. Chem.* **1996**, *35*, 5912.

(112) Drago, R. S.; Joerg, S. *J. Am. Chem. Soc.* **1996**, *118*, 2654.

(113) Glueck, D. S., Nolan, S. P. Unpublished information.

NaBH$_4$ and stored over activated 4Å molecular sieves. *p*-Toluidine, *p*-anisidine, and *p*-H$_2$NC$_6$H$_4$NMe$_2$ were sublimed prior to use. *m*-H$_2$-NC$_6$H$_4$F and *p*-H$_2$NC$_6$H$_4$CF$_3$ were dried over activated 4 Å sieves. *p*-Cresol and *p*-H$_2$NC$_6$H$_4$C(O)CH$_3$ were dried as benzene solutions over activated 4 Å molecular sieves, then filtered, and freeze-dried. *m*-H$_2$-NC$_6$H$_4$NMe$_2$ was isolated from its dihydrochloride by extracting with diethyl ether and aqueous KOH, drying over MgSO$_4$, and distilling from CaCl$_2$. Commercial Me$_3$SiH (Petrarch) as stored over NaOH or KOH to remove Me$_3$SiCl, which was present to the extent of 5−10%, as shown by ^{1}H NMR spectroscopy. Lithium amides were prepared by adding a slight deficiency of *n*-butyllithium or methyllithium (in hexanes or diethyl ether, respectively) to a hexanes or toluene solution of the appropriate amine, washing with hexanes or toluene, and removing volatile materials *in vacuo*. Benzylpotassium was prepared by a known method.[114] Cp*Ni(acac)[115] was synthesized according to published procedures,[32] as was Cp*Ni(PEt$_3$)Me.[22] All other starting materials were of reagent grade and were purified according to standard procedures, as necessary.[116] ^{1}H, ^{13}C{^{1}H}, and ^{31}P{^{1}H} NMR spectra were recorded on a Bruker AMX-400 spectrometer (100.6 MHz for carbon, 162.1 MHz for phosphorus). Chemical shifts are reported in parts per million (δ), coupling constants are reported in Hertz (Hz) and integrations are reported in number of protons. Unless otherwise indicated, ^{13}C{^{1}H} NMR resonances are singlets. Chemical shifts are referenced internally to the C$_6$D$_6$ solvent peaks at δ 7.15 (^{1}H) and 128.0 (^{13}C) ppm, the THF-d_8 solvent peaks at δ 3.58 (^{1}H) and 67.4 (^{13}C) ppm, or the CD$_2$Cl$_2$ solvent peaks at δ 5.31 (^{1}H) and 53.8 (^{13}C) ppm. In some cases, DEPT was used to assign the ^{13}C{^{1}H} NMR resonances as CH$_3$, CH$_2$, CH, or quaternary. IR spectra were recorded on a Mattson Galaxy Series FTIR 3000 spectrophotometer, as Nujol mulls on NaCl plates, as pressed KBr pellets, or as solutions between NaCl plates in a solution cell, and the frequencies are reported in cm^{-1}. UV/vis spectra were recorded at 298 K on solutions in quartz cuvettes (sealed to Kontes vacuum adapters), using a HP 8450A UV/vis spectrophotometer equipped with a temperature-control unit. Elemental analyses were performed at the UCB Microanalysis Facility; in the products of reactions where **1a** was a starting material, nitrogen was not detected (<0.1%).

Cp*Ni(PEt$_3$)OTf. In the glovebox, a solution of trifluoromethane-sulfonic (triflic) acid (0.13 mL, 1.5 mmol) in CH$_2$Cl$_2$ (7 mL) was added dropwise to a stirred solution of Cp*Ni(PEt$_3$)Me (469 mg, 1.43 mmol) in CH$_2$Cl$_2$ (15 mL), causing a change in color from green to burgundy. After 30 min of stirring, the volatile materials were removed *in vacuo*. The residue was extracted into diethyl ether (20 mL) and filtered to give a burgundy solution. The volume of the solution was reduced to 14 mL, and the solution was cooled to −30 °C, giving clumps of red crystals of Cp*Ni(PEt$_3$)OTf (261 mg, 39% yield). Collection of further crops of crystals was generally unsuccessful. ^{1}H NMR (CD$_2$Cl$_2$): δ 1.50 (m, 6, P(CH$_2$CH$_3$)$_3$), 1.41 (s, Cp*), 1.21 (m, 9, P(CH$_2$CH$_3$)$_3$). ^{13}C{^{1}H} NMR (CD$_2$Cl$_2$): δ 105.1 (C$_5$Me$_5$), 14.2 (d, J = 30 Hz, P(CH$_2$CH$_3$)$_3$), 10.2 (P(CH$_2$CH$_3$)$_3$), 7.9 (C$_5$Me$_5$). ^{31}P{^{1}H} NMR (CD$_2$Cl$_2$): δ 23.0. ^{19}F{^{1}H} NMR (CD$_2$Cl$_2$): δ −76.7. IR (Nujol): 2750 (w), 1535 (w), (1460−1370 obscured by Nujol), 1346 (m), 1288 (s), 1259 (s), 1223 (s), 1160 (s), 1106 (w), 1027 (s), 944 (w), 765 (m). Anal. Calcd: C, 44.28; H, 6.56. Found: C, 44.52; H, 6.64.

Cp*Ni(PEt$_3$)NHTol (1a). To a stirred solution of Cp*Ni(PEt$_3$)Me (1.64 g, 5.01 mmol) in CH$_2$Cl$_2$ (50 mL) was added a solution of triflic acid (0.52 mL, 5.89 mmol) in CH$_2$Cl$_2$ (25 mL). This caused a color change from pea-green to burgundy, as well as moderate effervescence. After the mixture was stirred for 15 min at ambient temperature, the volatile materials were removed *in vacuo* over several hours. The crude triflato complex was dissolved in THF (50 mL), and a solution of LiNHTol (692 mg, 6.12 mmol) in THF (30 mL) was added at 0 °C, giving an immediate color change to dark green. After the mixture was stirred for 10 min at 0 °C, the volatile materials were completely removed *in vacuo* at room temperature. The residue was extracted into pentane (4 × 20 mL); the resulting solution was filtered through

Celite (1 cm), reduced in volume to 25 mL, and slowly cooled to −80 °C. This gave large blue crystals of Cp*Ni(PEt$_3$)NHTol (1.15 g, 55% yield). ^{1}H NMR (C$_6$D$_6$): δ 6.95 (d, 2, J = 8 Hz, Tol aryl), 6.78 (d, 2, J = 8 Hz, Tol aryl), 2.32 (s, 3, Tol methyl), 1.54 (d, 15, J = 1.4 Hz, Cp*), 1.10 (m, 6, P(CH$_2$CH$_3$)$_3$), 0.87 (m, 9, P(CH$_2$CH$_3$)$_3$), −1.48 (s, 1, N*H*Tol). ^{13}C{^{1}H} NMR (C$_6$D$_6$): δ 157.9 (Tol quaternary), 129.5 (Tol methine), 118.0 (Tol methine), 117.6 (Tol quaternary), 100.5 (C$_5$Me$_5$), 20.8 (Tol methyl), 14.2 (d, J = 20 Hz, P(CH$_2$CH$_3$)$_3$), 10.4 (P(CH$_2$CH$_3$)$_3$), 7.7 (C$_5$Me$_5$). ^{31}P{^{1}H} NMR (C$_6$D$_6$): δ 25.1. IR (Nujol): ν_{NH} = 3333-(vw), 3323(vw). λ_{max} = 610 nm (ϵ (THF) = 1600 L/mol cm). Anal. Calcd: C, 66.05; H, 9.16; N, 3.35. Found: C, 66.01; H, 9.13; N, 3.17.

Complexes 1b, 1c, 1g. These compounds were not isolated; they were identified by their ^{1}H and ^{31}P NMR spectra in equilibration experiments. Cp*Ni(PEt$_3$)NH(*p*-C$_6$H$_4$NMe$_2$) (**1b**). ^{1}H NMR (C$_6$D$_6$): δ 2.69 (s, 3, NMe$_2$), 1.57 (d, 15, J = 1.4 Hz, Cp*), −1.67 (s, 1, NH). ^{31}P{^{1}H} NMR (C$_6$D$_6$): δ 25.1. Cp*Ni(PEt$_3$)NH(*p*-C$_6$H$_4$OMe) (**1c**). ^{1}H NMR (C$_6$D$_6$): δ 3.54 (s, 3, NMe$_2$), 1.55 (overlaps w/SM Cp*, Cp*), −1.67 (s, 1, NH). ^{31}P{^{1}H} NMR (C$_6$D$_6$): δ 25.2. Cp*Ni(PEt$_3$)NH(*m*-C$_6$H$_4$NMe$_2$) (**1g**). ^{1}H NMR (C$_6$D$_6$): δ 2.87 (s, 3, NMe$_2$), 1.56 (d, 15, J = 1.4 Hz, Cp*), −1.30 (s, 1, NH). ^{31}P{^{1}H} NMR (C$_6$D$_6$): δ 25.2.

Cp*Ni(PEt$_3$)NH(*p*-C$_6$H$_4$F) (1d). This amide was synthesized by a method analogous to that used for Cp*Ni(PEt$_3$)NHTol, giving a blue microcrystalline solid. ^{1}H NMR (C$_6$D$_6$): δ 6.87 (vt, 2, J$_{apparent}$ = 9 Hz, aryl), 6.59 (m, 2, aryl), 1.48 (d, 15, J = 1.4 Hz, Cp*), 1.06 (m, 6, P(CH$_2$CH$_3$)$_3$), 0.83 (m, 9, P(CH$_2$CH$_3$)$_3$), −1.54 (s, 1, N*H*Tol). ^{13}C{^{1}H} NMR (C$_6$D$_6$): δ 156.8 (*ipso* quaternary), 152.5 (d, J$_{CF}$ = 240 Hz, *para* quaternary), 117.1 (aryl methine), 115.0 (d, J$_{CF}$ = 20 Hz, aryl methine), 100.6 (C$_5$Me$_5$), 14.2 (d, J = 20 Hz, P(CH$_2$CH$_3$)$_3$), 10.3 (P(CH$_2$CH$_3$)$_3$), 7.6 (C$_5$Me$_5$). ^{31}P{^{1}H} NMR (C$_6$D$_6$): δ 25.2. ^{19}F{^{1}H} NMR (C$_6$D$_6$): δ −138.1. Anal. Calcd: C, 62.59; H, 8.36; N, 3.32. Found: C, 62.62; H, 8.45; N, 3.28.

Cp*Ni(PEt$_3$)NH(*p*-C$_6$H$_4$CF$_3$) (1e). A solution of *p*-trifluoromethylaniline (26 mg, 0.16 mmol) in diethyl ether (5 mL) was mixed with a solution of **3** (40.4 mg, 0.118 mmol) in diethyl ether (5 mL). The solution turned from orange-red to purple over ~30 s. After the mixture was stirred for 10 min, the volatile materials were removed *in vacuo* to give a quantitative yield of Cp*Ni(PEt$_3$)NH(*p*-C$_6$H$_4$CF$_3$). This material was crystallized from pentane before use to give spectroscopically pure material. In the ^{1}H NMR spectrum of this complex, the signals for the aryl group are broad due to fluxionality at room temperature; these peaks coalesced upon raising and decoalesced upon lowering the temperature. ^{1}H NMR (room temperature, C$_6$D$_6$): δ 7.5 (br, 2, aryl), 6.8 (br, 1, aryl), 6.3 (br, 1, aryl), 1.39 (d, 15, J = 1.5 Hz, Cp*), 0.98 (m, 6, P(CH$_2$CH$_3$)$_3$), 0.78 (m, 9, P(CH$_2$CH$_3$)$_3$), −0.52 (s, 1, N*H*). ^{13}C{^{1}H} NMR (C$_6$D$_6$, 345 K): δ 163.4 (aryl), 126.1 (aryl), amide ligand quaternary carbons not observed, 101.3 (C$_5$Me$_5$), 14.8 (d, J = 20 Hz, P(CH$_2$CH$_3$)$_3$), 10.2 (P(CH$_2$CH$_3$)$_3$), 7.5 (C$_5$Me$_5$). ^{31}P{^{1}H} NMR (C$_6$D$_6$): δ 25.6. ^{19}F{^{1}H} NMR (C$_6$D$_6$): δ −58.4.

Cp*Ni(PEt$_3$)NH(*m*-C$_6$H$_4$C(O)CH$_3$) (1f). A mixture of *p*-aminoacetophenone (8.5 mg, 0.063 mmol) and **3** (16.2 mg, 0.047 mmol) was dissolved in diethyl ether (10 mL). The color of the solution changed from red to purple over 1 min. Volatile materials were removed *in vacuo*, leaving a purple residue that was extracted with 1:1 pentane/ether (10 mL) and filtered. The solution was concentrated to 2 mL; pentane (5 mL) was added, and the solution was cooled to −30 °C, giving a purple microcrystalline solid. This solid was spectroscopically pure except for 0.1 equiv of excess *p*-aminoacetophenone (which is apparently not volatile enough for removal). Since this amine would be a component of equilibrium mixtures formed from the addition of TolNH$_2$ to **1f**, this was simply accounted for in K$_{eq}$ calculations. ^{1}H NMR (C$_6$D$_6$): δ 8.14 (br s, aryl), 7.75 (br s, aryl), 6.84 (br s, aryl), 6.26 (br s, aryl), 2.39 (s, 3, C(O)*Me*), 1.38 (d, 15, J = 1.5 Hz, Cp*), 0.03 (s, 1, NH). ^{31}P{^{1}H} NMR (C$_6$D$_6$): δ 25.7.

[Cp*Ni(PEt$_3$)$_2$][OTf]. A red solution of Cp*Ni(PEt$_3$)OTf was prepared by adding a solution of triflic acid (103 mg, 0.686 mmol) in dichloromethane (20 mL) to a green solution of Cp*Ni(PEt$_3$)Me (210 mg, 0.642 mmol) in dichloromethane (50 mL) at −78 °C. Triethylphosphine (0.10 mL, 0.68 mmol) was added to this solution via syringe. The solution was warmed to room temperature, and the solution turned orange over 12 h. After this time, all volatile materials were removed *in vacuo*. The brown residue was extracted with THF (10 mL) and filtered. The orange filtrate was concentrated to 7 mL, 4

(114) Schlosser, M.; Hartmann, J. *Angew. Chem., Int. Ed. Engl.* **1973**, *12*, 508.

(115) Bunel, E. E.; Valle, L.; Manriquez, J. M. *Organometallics* **1985**, *4*, 1680.

(116) Perrin, D. D.; Armarego, W. L. F. *Purification of Laboratory Chemicals*, 3rd ed.; Pergamon: New York, 1988.

mL of diethyl ether was added, and the solution was cooled to −30 °C. Two crops of brown crystals were obtained in this way in a total yield of 226 mg (61%). ^{1}H NMR (CD$_2$Cl$_2$): δ 1.68 (t, 15, J = 1.6 Hz, Cp*), 1.63 (m, 6, P(CH_2CH$_3$)$_3$), 1.09 (m, 9, P(CH$_2$CH_3)$_3$). ^{13}C-{^{1}H} NMR (THF-d_8): δ 106.6 (C_5Me$_5$), 13.6 (t, J = 14 Hz, P(CH$_2$-CH$_3$)$_3$), 11.4 (P(CH$_2$CH$_3$)$_3$), 8.3 (C_5Me$_5$). ^{31}P{^{1}H} NMR (CD$_2$Cl$_2$): δ 23.75. ^{19}F NMR (THF-d_8): δ −75.3. IR (Nujol): 2288 (w), 1455 (s), 1378 (s), 1351 (m), 1266 (s), 1224 (sh), 1146 (s), 1136 (m), 1030 (s), 944 (m), 757 (m), 714 (m), 705 (m), 673 (w), 636 (m), 615 (w). Anal. Calcd. for C$_{23}$H$_{45}$F$_3$NiO$_3$P$_2$S: C, 47.69; H, 7.83. Found: C, 47.91; H, 7.87.

(η^2-C$_5$Me$_4$CH$_2$)Ni(PEt$_3$)$_2$ (2). A solution of lithium diisopropyl-amide (38 mg, 0.35 mmol) in THF (5 mL) was added to a solution of [Cp*Ni(PEt$_3$)$_2$][OTf] (179 mg, 0.309 mmol) in THF (15 mL), causing a slight color change from yellow-brown to yellow-orange. After the mixture was stirred for 15 min, the volatile materials were removed *in vacuo*. The orange residue was extracted into pentane (1 mL) and filtered. Crystallization from this solvent did not occur, so the solution was extracted into (Me$_3$Si)$_2$O (1.5 mL) and cooled to −35 °C, giving **2** as an orange solid (64 mg, 48% yield). The solubility of this compound was similar to that of contaminants, so this solid was of ∼90% purity, sufficient for spectroscopic characterization. ^{1}H NMR (C$_6$D$_6$): δ 2.13 (s, 6, fulvene Me), 2.08 (d, 6, J = 3.0 Hz, fulvene Me), 2.05 (dd, 2, J = 5.9, 1 Hz, *exo* CH$_2$), 1.35 (m, 6, P(CH_2CH$_3$)$_3$), 1.09 (m, 6, P(CH$_2$CH$_3$)$_3$), 0.93 (m, 9, P(CH$_2$CH_3)$_3$), 0.84 (m, 9, P(CH$_2$CH_3)$_3$). ^{13}C{^{1}H} NMR (C$_6$D$_6$, for assignments, compare to the Pd analogue[29]): δ 128.5 (dd, J = 4, 2 Hz), 126.2 (d, J = 3 Hz), 83.0 (d, J = 10 Hz), 31.5 (d, J = 17 Hz, methylene), 19.1 (dd, J = 17, 3 Hz, methylene), 15.3 (dd, J = 17, 2 Hz, methylene), 12.5 (s), 12.0 (s), 8.8 (s), 8.3 (s). ^{31}P{^{1}H} NMR (C$_6$D$_6$): δ 21.6 (d, J = 40 Hz), 14.1 (d, J = 40 Hz). IR (Nujol): 2731 (w), 1523 (m), 1375 (s), 1336 (s), 1252 (m), 1178 (m), 1149 (w), 1034 (s), 997 (m), 943 (m), 885 (m), 760 (s), 710 (s), 663 (m), 617 (m). High-resolution EI-MS (found/calcd for NiP$_2$C$_{22}$H$_{44}$): 431.226 643/431.225 972, 430.223 262/430.222 618, 429.231 032/429.230 530, 428.227 093/428.227 176.

Cp*Ni(PEt$_3$)OMe (3). A solution of triflic acid in methanol (3.7 mL, 0.35 M) was added to a stirred solution of Cp*Ni(PEt$_3$)Me (197 mg, 0.602 mmol) in methanol (20 mL). This caused the color to change from green to burgundy. A solution of NaOMe, prepared by adding MeOH (10 mL) to elemental sodium (42.4 mg), was added to the burgundy solution of nickel triflate. The volatile materials were removed from the resulting red solution *in vacuo*. The red-brown residue was extracted with 20 mL of pentane, filtered through a pad of Celite, and concentrated to 5 mL in vacuo. Hexamethyldisiloxane (1 mL) was added, and the solution was filtered again and cooled to −30 °C. Three crops of red-orange crystals were collected in a total yield of 109 mg (53%). ^{1}H NMR (C$_6$D$_6$): δ 3.32 (s, 3, OCH_3), 1.61 (d, 15, J = 1.3 Hz, Cp*), 1.28 (m, 6, P(CH_2CH$_3$)$_3$), 1.05 (m, 9, P(CH$_2$CH_3)$_3$). ^{13}C{^{1}H} NMR (C$_6$D$_6$): δ 99.9 (C_5Me$_5$), 57.9 (OMe), 13.6 (d, J = 20 Hz, P(CH$_2$CH$_3$)$_3$), 10.3 (P(CH$_2$CH$_3$)$_3$), 8.0 (C_5Me$_5$). ^{31}P{^{1}H} NMR (C$_6$D$_6$): δ 25.0. IR (C$_6$D$_6$): 2749 (m), 1065 (s), 1034 (m), 764 (m), 720 (m). Anal. Calcd: C, 59.51; H, 9.69. Found: C, 59.59; H, 9.70.

Generation of "Cp*Ni(PEt$_3$)OH". A solution of **1** (2 mg, 0.005 mmol) in C$_6$D$_6$ (0.6 mL) was placed in an NMR tube that was capped with a septum. Degassed water (1.0 μL, 0.056 mmol) was added via syringe, and the mixture was shaken vigorously for 3 min. The solution turned to an orange-yellow color; ^{1}H NMR spectroscopy showed one new product, along with 1 equiv of TolNH$_2$, excess water (δ 5.3 ppm (br)), and a small amount (∼5%) of the starting amido complex. For "Cp*Ni(PEt$_3$)OH": ^{1}H NMR (C$_6$D$_6$): δ 1.41 (s, 15, Cp*), 1.24 (m, 6, P(CH_2CH$_3$)$_3$), 0.99 (m, 9, P(CH$_2$CH_3)$_3$), OH not detected. ^{31}P{^{1}H} NMR (C$_6$D$_6$): δ 24.3.

Adsorption and Removal of [Cp*Ni(PEt$_3$)] on Silica. A solution of **1a** (25.4 mg, 0.0607 mmol) in diethyl ether (4 mL) was passed through a column of dried silica in a disposable pipet (5 cm), causing the silica to turn red. The column was rinsed with diethyl ether (3 mL) and THF (3 mL). The eluent was dried *in vacuo*, leaving 7.0 mg of a tan residue (>90% toluidine by ^{1}H NMR spectroscopy; theoretical yield = 6.5 mg; >95% yield of TolNH$_2$). A solution of *p*-nitrophenol (9.2 mg, 1.1 equiv) in THF (1 mL) was passed through the column of red silica three times; after this treatment the solution was orange-red, and the silica remained tan. The column was rinsed with 2 mL of

pure THF; however, the silica did not return to white. The combined washings were dried in vacuo to give an orange solid (25.8 mg, 85:15 ratio of nickel phenolate to phenol by ^{1}H NMR spectroscopy; 90% yield of nickel phenolate). For Cp*Ni(PEt$_3$)OC$_6$H$_4$NO$_2$: ^{1}H NMR (C$_6$D$_6$): δ 8.24 (d, 2, J = 7.2 Hz, aryl), 6.81 (d, 2, J = 7.2 Hz, aryl), 1.21 (d, 15, J = 1.5 Hz, Cp*), 0.93 (m, 6, P(CH_2CH$_3$)$_3$), 0.82 (m, 9, P(CH$_2$CH_3)$_3$). ^{31}P{^{1}H} NMR (C$_6$D$_6$): δ 21.9.

Cp*Ni(PEt$_3$)OTol (4). Complex **1a** (355 mg, 0.850 mmol) and *p*-cresol (92.1 mg, 0.852 mmol) were placed in a flask. Diethyl ether (10 mL) was added, and the solution rapidly changed color from blue-purple to deep red. After the mixture was stirred for 15 min at ambient temperature, the volatile materials were removed *in vacuo* and the residue was exposed to high vacuum (∼1 mTorr) overnight. The red residue was extracted into pentane (12 mL), filtered, reduced in volume to 8 mL, and cooled to −30 °C. This gave red crystals of Cp*Ni-(PEt$_3$)OTol (299 mg, 84% yield). ^{1}H NMR (C$_6$D$_6$): δ 7.17 (d, 2, J = 8 Hz, Tol aryl), 7.04 (d, 2, J = 8 Hz, Tol aryl), 2.31(s, 3, Tol methyl), 1.43 (s, 15, J = 1.4 Hz, Cp*), 1.13 (m, 6, P(CH_2CH$_3$)$_3$), 0.96 (m, 9, P(CH$_2$CH_3)$_3$). ^{13}C{^{1}H} NMR (C$_6$D$_6$): δ 166.5 (Tol quaternary), 129.4 (Tol methine), 121.8 (Tol methine), 120.6 (Tol quaternary), 101.5 (C_5-Me$_5$), 20.7 (Tol methyl), 14.0 (d, J = 20 Hz, P(CH$_2$CH$_3$)$_3$), 10.3 (P(CH$_2$CH$_3$)$_3$), 7.6 (C_5Me$_5$). ^{31}P{^{1}H} NMR (C$_6$D$_6$): δ 21.8. λ_{max}: 540 nm (ϵ (THF) = 725 L/mol cm). Anal. Calcd: C, 65.90; H, 8.90. Found: C, 65.93; H, 9.04.

Cp*Ni(PEt$_3$)STol (5). A mixture of **1a** (26.0 mg, 0.0622 mmol) and *p*-thiocresol (8.7 mg, 0.070 mmol, 1.1 equiv) was dissolved in diethyl ether (5 mL). The color of the solution rapidly changed from blue to brown. This solution was exposed to vacuum overnight to remove solvent, *p*-toluidine, and excess *p*-thiocresol. The residue was extracted with pentane (5 mL) and filtered. The green-brown filtrate was concentrated to 1 mL and cooled to −30 °C, giving green blocks of **5**. Collection of an additional crop of crystals from hexamethyldi-siloxane (1 mL) gave a total yield of 22 mg (81%). ^{1}H NMR (C$_6$D$_6$): δ 7.84 (d, 2, J = 8 Hz, Tol aryl), 6.90 (d, 2, J = 8 Hz, Tol aryl), 2.17(s, 3, Tol methyl), 1.62 (d, 15, J = 1.3 Hz, Cp*), 1.32 (m, 6, P(CH_2-CH$_3$)$_3$), 0.84 (m, 9, P(CH$_2$CH_3)$_3$). ^{13}C{^{1}H} NMR (C$_6$D$_6$): δ 144.5 (Tol quaternary), 132.6 (Tol methine), 129.7 (Tol quaternary), 128.3 (Tol methine), 101.5 (C_5Me$_5$), 20.9 (Tol methyl), 15.1 (d, J = 20 Hz, P(CH$_2$-CH$_3$)$_3$), 10.6 (P(CH$_2$CH$_3$)$_3$), 7.9 (C_5Me$_5$). ^{31}P{^{1}H} NMR (C$_6$D$_6$): δ 25.0. IR (Nujol): 1893 (w), 1880 (w), 1713 (w), 1639 (w), 1596 (s), 1349 (s), 1246 (s), 1157 (s), 1083 (s), 1029 (s), 1001 (sh), 944 (m), 833 (w), 804 (s), 762 (s), 715 (s), 671 (m), 629 (m). Anal. Calcd: C, 63.46; H, 8.57. Found: C, 63.38; H, 8.67.

Cp*Ni(PEt$_3$)SC$_6$H$_4$CF$_3$ (5-F$_3$). To a solution of Cp*Ni(PEt$_3$)Me (31.2 mg, 0.095 mmol) in diethyl ether (2 mL) was added a solution of *p*-(trifluoromethyl)thiophenol (21.7 mg, 0.122 mmol) in diethyl ether (1 mL). Over a few min, the solution turned from green to rust-orange. The solution was heated to 45 °C for 33 h, after which time it was dark red. The volatile materials were removed *in vacuo*, and the brown-red residue was warmed to 60 °C under vacuum to remove excess thiol. Finally, the residue was extracted with pentane (4 mL), filtered, concentrated to 1 mL, and cooled to −30 °C, giving red-brown crystals (23.3 mg, 50%). The high solubility of the product hampered attempts to isolate further crystals. ^{1}H NMR (C$_6$D$_6$): δ 7.82 (d, 2, J = 8 Hz, Tol aryl), 7.28 (d, 2, J = 8 Hz, Tol aryl), 1.51 (s, 15, Cp*), 1.21 (m, 6, P(CH_2CH$_3$)$_3$), 0.75 (m, 9, P(CH$_2$CH_3)$_3$). ^{31}P{^{1}H} NMR (C$_6$D$_6$): δ 25.1. ^{19}F NMR (C$_6$D$_6$): δ −60.96. Anal. Calcd: C, 56.46; H, 7.00. Found: C, 56.35; H, 7.13.

Cp*Ni(PEt$_3$)H (6). Complex **1a** (520 mg, 1.24 mmol) was dissolved in benzene (15 mL) and placed in a 50 mL reaction tube. The solution was frozen and the headspace was evacuated. Trimethylsilane (505.7 mL at 666 Torr, 18 mmol) was condensed into the tube. The tube was then closed and warmed to room temperature for 1 d; over this time, the color changed slowly from blue to brown. The volatile materials were removed *in vacuo*, and the tube was placed under dynamic vacuum (∼10^{-4} Torr) overnight. The brown residue was extracted with pentane (10 mL), filtered, concentrated to 1 mL *in vacuo*, and cooled to −30 °C. Two crops of brown crystals were collected for a total yield of 377 mg (97%). ^{1}H NMR (C$_6$D$_6$): δ 2.06 (s, 15, no coupling resolved, Cp*), 1.16 (m, 6, P(CH_2CH$_3$)$_3$), 0.88 (m, 9, P(CH$_2$CH_3)$_3$), −21.4 (d, 1, J = 105 Hz, Ni-H). ^{13}C{^{1}H} NMR (C$_6$D$_6$): δ 96.8 (C_5Me$_5$), 20.5 (d, J = 30 Hz, P(CH_2CH$_3$)$_3$), 11.8

(P(CH$_2$CH$_3$)$_3$), 8.4 (C$_5$Me$_5$). ^{31}P NMR{^{1}H} (C$_6$D$_6$): δ 38.0 (s). IR (C$_6$D$_6$): 1894 (vs), 1468 (m), 1414 (m), 1375 (m), 1249 (m), 1034 (s), 766 (s), 722 (s), 627 (m). Anal. Calcd: C, 61.38; H, 9.98. Found: C, 61.26; H, 10.05.

Cp*Ni(PEt$_3$)Cl. Chlorotrimethylsilane (0.15 mL, 1.2 mmol, 11 equiv) was added to a solution of **1a** (46 mg, 0.11 mmol) in diethyl ether (5 mL). Over 2 h, the solution turned from blue to red. Volatile materials were removed *in vacuo*, and the residue was redissolved in ether (10 mL), filtered, concentrated to 2 mL, and cooled to −30 °C. This gave small red blocks (29 mg, 76%) of analytical purity. ^{1}H NMR (C$_6$D$_6$): δ 1.45 (s, 15, Cp*), 1.33 (m, 6, PCH_2CH$_3$), 0.96 (m, 9, PCH$_2$CH_3). ^{13}C{^{1}H} NMR (C$_6$D$_6$): δ 102.6 (Cp* quaternary), 15.0 (d, $J = 30$ Hz, P(CH$_2$CH$_3$)$_3$), 10.4 (P(CH$_2$CH$_3$)$_3$), 8.1 (C$_5$Me$_5$). ^{31}P-{^{1}H} NMR (C$_6$D$_6$): δ 22.95. IR (C$_6$D$_6$): 2964 (s), 2910 (s), 2875 (m), 1462 (w), 1415 (m), 1377 (m), 1347 (w), 1330 (w), 1249 (w), 1035 (s), 764 (s), 720 (s), 554 (s). Anal. Calcd for C$_{16}$H$_{30}$ClNiP: C, 55.29; H, 8.70. Found: 55.25; H, 8.85.

Cp*Ni(PEt$_3$)CH$_2$Ph. A red solution of KCH$_2$Ph (21.3 mg, 0.164 mmol) in THF (4 mL) was added to a blue solution of **1a** (65 mg, 0.155 mmol) in THF (4 mL). The mixture immediately turned green-brown. After the mixture was stirred for 1 h, the volatile materials were removed *in vacuo*. The residue was extracted with 8 mL pentane and filtered through a pad of Celite. The green filtrate was determined to be >98% pure by ^{1}H and ^{31}P NMR spectroscopy. Analytically pure material could be obtained by crystallization from pentane. ^{1}H NMR (C$_6$D$_6$): δ 7.39 (d, 2, $J = 7$ Hz, Ph), 7.11 (t, 2, $J = 8$ Hz, Ph), 6.90 (m, 1, Ph), 1.75 (d, 15, $J = 0.8$ Hz, Cp*), 1.37 (d, 2, $J = 6$ Hz, Ni-CH_2), 0.98 (m, 6, P(CH_2CH$_3$)$_3$), 0.75 (m, 9, P(CH$_2$CH_3)$_3$). ^{13}C{^{1}H} NMR (C$_6$D$_6$): δ 153.6 (Ph quaternary), 129.7 (Ph methine), 127.5 (Ph methine), 122.5 (Tol methine), 98.7 (C$_5$Me$_5$), 13.9 (d, $J = 20$ Hz, P(CH$_2$-CH$_3$)$_3$), 10.7 (P(CH$_2$CH$_3$)$_3$), 7.7 (C$_5$Me$_5$), 3.9 (d, $J = 20$ Hz, Ni-CH$_2$). ^{31}P{^{1}H} NMR (C$_6$D$_6$): δ 29.4. IR (Nujol): 1592 (m), 1157 (m), 1035 (s), 1025 (s), 763 (s), 750 (s), 715 (s), 699 (s). Anal. Calcd: C, 68.51; H, 9.25. Found: C, 68.44; H, 9.49.

(DPPE)Pt(Me)(O(p-C$_6$H$_4$Me)). A solution of *p*-cresol (5.6 mg, 52 μmol) in CH$_2$Cl$_2$ (2 mL) was added to a solution of (DPPE)Pt(Me)-(OH)·C$_6$H$_6$[117] (35.2 mg, 50.0 μmol) in CH$_2$Cl$_2$ (1 mL) and stirred for 1.5 d. The volatile materials were removed *in vacuo*, and the residue was treated with benzene and then evaporated several times to remove water. This residue was dissolved in CH$_2$Cl$_2$/ether; vapor diffusion of pentane into this solution gave pale yellow crystals of (DPPE)Pt(Me)-(O(p-C$_6$H$_4$Me)) (24 mg, 67% yield). ^{1}H NMR (THF-d_8): δ 7.98 (m, 4, Ph), 7.75 (m, 4, Ph), 7.45 (m, 6, Ph), 7.32 (m, 6, Ph), 6.63 (d, 2, $J = 8.4$ Hz, Tol), 6.57 (d, 2, $J = 8.4$ Hz, Tol), 2.45 (m, 2, PCH$_2$CH$_2$P), 2.24 (m, 2, PCH$_2$CH$_2$P), 2.09 (s, 3, Tol), 0.42 (dd, 3, $J = 2.9, 7.8$ Hz, Pt-*Me*). ^{31}P{^{1}H} NMR (THF-d_8): δ 45.14 ($J_{Pt-P} = 1764$ Hz), 39.24 ($J_{Pt-P} = 3811$ Hz).

(DPPE)Pt(Me)(NH(p-C$_6$H$_4$Me)). This uses the method of Bryndza *et al.*[72] A flask was charged with LiNH(p-C$_6$H$_4$Me) (17 mg, 150 μmol), (DPPE)Pt(Me)(Cl)[118] (78 mg, 121 μmol) and a stir bar and capped with a vacuum adapter. The flask was cooled to −196 °C, THF (8 mL) was condensed into the flask, and the yellow solution was slowly warmed to room temperature. After the mixture was stirred for 10 min at room temperature, the volatile materials were removed *in vacuo*. In the glovebox, the residue was extracted with benzene (6 mL), filtered through a Celite pad, and the solvent was evaporated to leave a fluffy yellow powder of (DPPE)Pt(Me)(NH(p-C$_6$H$_4$Me)) (81 mg, 94% yield). This material was not completely pure, but was used for spectral comparisons only. ^{1}H NMR (THF-d_8): δ 7.83 (m, 4, Ph), 7.76 (m, 4, Ph), 7.44 (m, 6, Ph), 7.35 (m, 6, Ph), 6.38 (d, 2, $J = 8.2$ Hz, Tol), 6.22 (d, 2, $J = 8.3$ Hz, Tol), 2.39 (m, 2, PCH$_2$CH$_2$P), 2.19 (m, 2, PCH$_2$-CH$_2$P), 2.00 (s, 3, Tol), 0.54 (dd, 3, $J = 4.8, 7.6$ Hz, Pt-*Me*). ^{31}P{^{1}H} NMR (THF-d_8): δ 44.95 ($J_{Pt-P} = 1729$ Hz), 44.69 ($J_{Pt-P} = 3145$ Hz).

Equilibrium Measurements by NMR Spectroscopy. In a typical experiment, **1a** (10.7 mg, 25.6 μmol) and *m*-H$_2$NC$_6$H$_4$NMe$_2$ (4.7 mg, 35 μmol) were weighed into a vial. This mixture was dissolved in C$_6$D$_6$ (0.5 mL), and the resulting blue solution was placed in a J. Young NMR tube. The solution was monitored by ^{1}H and ^{31}P NMR spectroscopy, which indicated that equilibrium had been reached in

several hours. Although this equilibration rate was typical for most substituted anilines, the equilibration time for the aryloxide was only a few minutes, while the equilibration took several days in the case of Cp*Ni(PEt$_3$)NH(p-C$_6$H$_4$CF$_3$) + TolNH$_2$. The ratios of the amines and amides were determined by integration of one-pulse ^{1}H NMR spectra and of ^{31}P NMR spectra; the error was estimated from the variance of the ratios using different peaks. For this equilibrium, the final relative ratio [**1a**]: [Cp*Ni(PEt$_3$)NHAr] = [TolNH$_2$]: [*m*-H$_2$NC$_6$H$_4$NMe$_2$] was 1:1.55 ($\pm$0.05):2.2 ($\pm$0.1); thus, $K_{eq} = 1.1 \pm 0.1$. Errors were estimated from the range of measured K_{eq} values. A list of equilibration times and K_{eq} values for the various equilibria is in the Supporting Information.

Equilibrium Measurements by UV/Vis Spectroscopy. The extinction coefficients (at 500, 538, 608, and 690 nm) for **1a**, **4**, and TolNH$_2$ were derived from successive dilution of solutions having roughly the molarity used in the equilibrium experiments. Linear plots verified that Beer's Law holds in the concentration regime used. In the actual equilibrium experiments, measured volumes of solutions of **4** and TolNH$_2$ were mixed, and the absorbances at 500, 538, 608, and 690 nm were monitored. These approached equilibrium values over a few hours, and eventually began dropping, presumably due to decomposition. Equilibrium constants were calculated from the equilibrium absorbances at each wavelength monitored; however, reproducible values were found only using the high-wavelength absorbance values (608 and 690 nm). The equations used to derive equilibrium constants (A = absorbance) at each wavelength were

$$[\mathbf{1a}]_{eq} = (A - (\epsilon_4[\mathbf{4}]_o) - (\epsilon_{TolNH_2}[TolNH_2]_o))/(\epsilon_{1a} - \epsilon_4) \quad (11)$$

$$K_{eq} = [\mathbf{1a}]_{eq}^2/([TolNH_2]_o)([\mathbf{4}]_o - [\mathbf{1a}]_{eq}) \quad (12)$$

Thus, the change in the small absorbance of the organic molecules in the visible region was ignored.

The experiment was repeated using several different [**4**]$_o$ and [TolNH$_2$]$_o$ in order to gauge reproducibility. The concentrations and K_{eq} values used may be found in the Supporting Information. Errors were estimated from the variance in K_{eq} values derived from eqs 11 and 12, as the standard deviation ($\sim$70% confidence).

Phosphine Exchange Kinetics. In the glovebox, a solution of Cp*Ni(PEt$_3$)X (2 mg) in C$_6$D$_6$ (0.5 mL) was placed in a J. Young NMR tube and degassed. An aliquot of trimethylphosphine at known pressure in a bulb of known volume was condensed into the NMR tube at 77 K. The sample was placed in an NMR probe (300 MHz) at the appropriate temperature (X = OTol: 235 $\pm$ 3 K;[119] X = STol, SC$_6$H$_4$-CF$_3$: 31.7 $\pm$ 0.1 °C), and one-pulse spectra were acquired every 2 min (X = OTol), 3 min (X = OTol), or 6 min (X = SAr) for several hours; in each case, the reaction was monitored over at least 3 half-lives. The spectra were integrated, and the integrations for the Cp* methyl resonances (X = SAr) or the tolyl methyl resonances (X = OTol) were plotted and fit using KaleidaGraph. Error limits are derived from Kaleidagraph's curve-fitting procedures. Phosphine concentrations were derived from integration of the NMR spectra, and were corrected for the volume of trimethylphosphine.

X-ray Crystal Structure of 1a. General procedures for crystallography on the CAD4 system at Berkeley have been given previously;[120] parameters specific to this data set are given in Table 4. Automatic peak search and indexing procedures yielded a monoclinic reduced primitive cell. Inspection of the Niggli values revealed a potential C-centered orthorhombic unit cell, but inspection of the data showed only monoclinic symmetry. Inspection of the intensity standards revealed a reduction of 6.6% of the original intensity; the data were corrected for this decay. Inspection of the azimuthal scan data showed a variation $I_{min}/I_{max} = 0.72$ for the average curve. However, the curves clearly showed that the crystal was not well-oriented at the time of the collection. An empirical correction was made to the data on the basis of the combined differences of F_{obs} and F_{calc} following refinement of all atoms with isotropic thermal parameters ($T_{max} = 1.20$, $T_{min} = 0.87$, no θ dependence). Inspection of the

(117) Appleton, T. G.; Bennett, M. A. *Inorg. Chem.* **1978**, *17*, 738.
(118) Clark, H. C.; Jablonski, C. R. *Inorg. Chem.* **1975**, *14*, 1518.

(119) Although the absolute temperature is not known to an *accuracy* of better than $\pm$3 K, the temperature was maintained to $\pm$0.1 K within each kinetic run using **4**.
(120) Dobbs, D. A.; Bergman, R. G. *Inorg. Chem.* **1994**, *33*, 5329.

Table 4. Crystal and Data Parameters for **1a** and **4·HOXyl**

compound	1a	4·HOXyl
crystal dimensions (mm)	0.25 × 0.27 × 0.45	0.32 × 0.19 × 0.10
reflections for cell determination	24 (26° < θ < 30°)	8752 with $I > 10\sigma(I)$
a (Å)	16.639(3)	11.4752(3)
b (Å)	16.648(3)	13.7416(3)
c (Å)	16.615(3)	18.8274(5)
β (deg)	91.615(3)	99.734(1)
V (Å^3)	4600.5(25)	2926.1(1)
space group	$P2_1/c$ (no. 14)	$P2_1/c$ (no. 14)
Z	8	4
μ_{calc} (Mo Kα, cm^{-1})	9.2	7.43
T (°C)	−102	−141
frame time (s)	N/A	30
no. of reflections	6246	11986
no. of unique reflections	5987	4384 (R_{int} = 4.3%)
T_{min}, T_{max}	1.20, 0.87	0.990, 0.834
no. observations ($I > 3\sigma(I)$)	4059	3332
no. variables	469	459
R; R_w	0.047, 0.056	0.030, 0.039
R (including zeros)	0.082	0.040
goodness of fit indicator	1.50	1.43

Table 5. Calorimetric Enthalpies for Reaction and Solution in C$_6$H$_6$ at 30 °C

complex	solvent + reactant	ΔH (kcal/mol)
1a	C$_6$H$_6$	6.5 (0.2)
1a	C$_6$H$_6$ + TolOH	−2.9 (0.2)
1a	C$_6$H$_6$ + TolSH	−16.5 (0.2)
4	C$_6$H$_6$	4.6 (0.2)
4	C$_6$H$_6$ + TolSH	−9.4 (0.1)

systematic absences indicated uniquely space group $P2_1/c$. Hydrogen atoms were assigned idealized locations and values of B_{iso} approximately 1.25 times the B_{eq} of the atoms to which they were attached. The amino hydrogens were located on a difference Fourier map prior to their inclusion in calculated positions. All hydrogens were included in structure factor calculations, but not refined. Final agreement factors are as follows: R = 4.7%, wR = 5.6%, and GOF = 1.50; using all unique data, R = 8.15%. The largest peak in the final difference Fourier map had an electron density of 0.52 e^-/Å^3, and the lowest excursion −0.15 e^-/Å^3.

X-ray Crystal Structure of 4·HOXyl. General procedures for crystallography on the SMART/CCD system with integration and solution using SAINT and teXsan, respectively, are given in the accompanying paper;[22] parameters specific to this data set are given in Table 4. Red plates were obtained by cooling a pentane solution containing equimolar amounts of **4** and HOXyl to −30 °C. A semiempirical ellipsoidal absorption correction (T_{max} = 0.990, T_{min} = 0.834) was applied to the raw data. Equivalent reflections were averaged. The non-hydrogen atoms were refined anisotropically. The hydrogen atoms were located in Fourier syntheses and their positions were refined in the final stages of refinement, using fixed isotropic thermal parameters of approximately 1.2 times that of the atom to which they were attached. Because of the high quality of the data set, it was possible to refine the hydrogen-bonding hydrogen atom isotropically; the value of B_{iso} = 3.3 for this atom shows that this model behaved well. Final agreement factors are as follows: R = 3.0%, R_w = 3.9%, and GOF = 1.43; using all unique data, R = 4.0%, R_w = 4.2%.

Calorimetry. Only materials of high purity as indicated by IR and NMR spectroscopies were used in the calorimetric experiments. Calorimetric measurements were performed using a Calvet calorimeter (Setaram C-80) which was periodically calibrated using the TRIS reaction[121] or the enthalpy of solution of KCl in water.[122] The experimental enthalpies for these two standard reactions compared very closely to literature values. This calorimeter has been previously described[123] and typical procedures are described below. Experimental enthalpy data (Table 5) are reported with 95% confidence limits.

NMR Titrations. Prior to every set of calorimetric experiments involving a new ligand, an accurately weighed amount (±0.1 mg) of

the organometallic complex was placed in a Wilmad screw-capped NMR tube fitted with a septum, and C$_6$D$_6$ was subsequently added. The solution was titrated with a solution of the ligand of interest by injecting the latter in aliquots through the septum with a microsyringe, followed by vigorous shaking. The reactions were monitored by ^{31}P and ^{1}H NMR spectroscopy and were found to be rapid, clean, and quantitative under experimental calorimetric conditions. These conditions are necessary for accurate and meaningful calorimetric results and were satisfied for all organometallic reactions investigated.

Calorimetric Measurement for Reaction between 1a and TolOH. The mixing vessels of the Setaram C-80 were cleaned, dried in an oven maintained at 120 °C, and then taken into the glovebox. A 20 mg sample of **1a** was accurately weighed into the lower vessel, closed, and sealed with 1.5 mL of mercury. Four milliliters of 1 equiv stock solution of cresol (26 mg of cresol in 20 mL of C$_6$H$_6$) was added and the remainder of the cell was assembled, removed from the glovebox and inserted in the calorimeter. The reference vessel was loaded in an identical fashion with the exception that no organonickel complex was added to the lower vessel. After the calorimeter had reached thermal equilibrium (about 2 h) the reactants were mixed by inverting the calorimeter, and the vessel was then allowed to return to equilibrium. Then, the vessels were removed from the calorimeter, taken into the glovebox, opened, and analyzed using ^{1}H NMR spectroscopy. Conversion to **4** was found to be quantitative under these reaction conditions. The enthalpy of reaction, −2.9 ± 0.2 kcal/mol, represents the average of five individual calorimetric determinations. The enthalpy of solution of **1a** was then subtracted from this value to obtain a value of −9.4 ± 0.3 kcal/mol for an enthalpy of reaction with all species in solution.

Calorimetric Measurement of Enthalpy of Solution of 1a in C$_6$H$_6$. This was performed by using a similar procedure as the one described above with the exception that no TolOH was added to the reaction cell. This enthalpy of solution, representing the average of five individual determinations, was measured as 6.5 ± 0.2 kcal/mol.

Supporting Information Available: Data from equilibration experiments, and tables of crystal structure determination data for **1a** and **4·HOXyl** (10 pages). See any current masthead page for ordering and Internet access instructions.

JA971829P

(121) Ojelund, G.; Wadsö, I. *Acta Chem. Scand.* **1968**, *22*, 1691.
(122) Kilday, M. V. *J. Res. Natl. Bur. Stand. (U.S.)* **1980**, *85*, 467.

(123) (a) Nolan, S. P.; Hoff, C. D.; Landrum, J. T. *J. Organomet. Chem.* **1985**, *282*, 357. (b) Nolan, S. P.; Lopez de la Vega, R.; Hoff, C. D. *Inorg. Chem.* **1986**, *25*, 4446.